

Internal evolution of the Tin Mountain pegmatite, Black Hills, South Dakota

RICHARD J. WALKER,* G. N. HANSON

Department of Earth and Space Sciences, State University of New York, Stony Brook, New York 11794

J. J. PAPIKE

Institute for the Study of Mineral Deposits, South Dakota School of Mines and Technology, Rapid City, South Dakota 57701

J. R. O'NEIL

U.S. Geological Survey, Menlo Park, California 94025

J. C. LAUL

Radiological Sciences Department, Battelle Northwest, Richland, Washington 99352

ABSTRACT

Major and trace elements and oxygen-isotope compositions are evaluated to delineate the sequence of crystallization in the lithologically and chemically zoned Tin Mountain pegmatite. The pegmatite consists of four stacked tabular zones surrounded by an enclosing wall zone. Each zone is lithologically, compositionally and texturally distinct, although intrazone contacts are gradational. Oxygen-isotope geothermometry, rare-earth-element patterns, low concentrations of Rb, Cs, and Li, and high concentrations of Ba and Sr in the wall zone indicate that it crystallized first. Cooling trends indicated by two-feldspar geothermometry, the presence of positive Eu anomalies in feldspars, and low concentrations of Rb and Cs in the uppermost inner zone suggest that it crystallized next. The three remaining lower zones then crystallized simultaneously. It is suggested that an aqueous-fluid film connected all crystallization fronts in the body. This aqueous fluid vertically redistributed Si, Al, K, Na, and possibly Rb and Cs in such a manner that the melt retained a ternary-minimum melt composition throughout crystallization.

INTRODUCTION

A framework in which to examine the internal evolution of pegmatites was proposed by Jahns and Burnham (1969) and has been subsequently updated and modified by Uebel (1977), Jahns (1982), and Norton (1983). In studies by Weis (1953), Staatz et al. (1955), Orville (1960), and Norton et al. (1962), for example, petrography and compositional variations of mineral and whole-rock samples were examined to better understand pegmatite petrogenesis and crystallization trends. In combination with experimental results, most of these studies indicate that (1) zoned pegmatites crystallize from a silicate melt from outer shell to center and (2) an aqueous fluid is exsolved at some stage during the crystallization. These conclusions are supported by the more recent studies employing radiogenic and stable isotope and trace-element measurements (Brookins, 1969; Register, 1979; Taylor and Friedrichsen, 1983a, 1983b; Černý et al., 1984). Few studies, however, have documented the crystallization paths of zoned pegmatites, or proposed adequate models to explain the presence of lithologic zonations. In this study, the crystallization path of the zoned Tin Mountain pegmatite is examined using major-element, trace-element, and oxygen-isotope compositions, and a crystallization sequence

is suggested. Processes consistent with this crystallization sequence that may have caused the zonation are discussed.

ANALYTICAL PROCEDURES

Mineral separates were obtained by a combination of magnetic and heavy-liquid separation and hand picking. Powders were sieved to less than 200 mesh and homogenized before dissolution. Two whole-rock samples of wall zone (9-2 and 10-3) were powdered from 5 kg of rock. A sample of the wall zone, 43-1, was produced by homogenization of approximately 100 kg of rock.

Rare-earth-element (REE) concentrations were determined by isotope dilution. Powders were prespiked with a multi-REE spike. The mineral separates intended for REE separation were dissolved by reaction of approximately 2 g of sample with a mixture of HF and HNO₃ in teflon reaction vessels heated to 205°C for at least 12 h. Whole-rock samples of about 200 mg were dissolved in 800 mg of LiBO₂ flux heated to 1050°C. REE separation procedures are described in Shirey (1984).

Isotope-dilution measurements were made using an automated 15-cm-radius NBS-designed mass spectrometer employing a single tantalum filament for ionization of REE from Ce to Eu. A 30-cm-radius NBS-designed mass spectrometer was used for measuring REE from Gd to Yb, which were ionized using triple Re filaments. Analyses of whole-rock samples and apatite separates generally reproduce to better than 2% for all REE. Analyses of samples

* Present address: National Bureau of Standards, Gaithersburg, Maryland 20899.

with less than 30 ppb Nd, however, varied by as much as 30%, although pattern shapes varied little. This lower precision may be attributed to heterogeneity in the sample due to the possible presence of micro-inclusions of apatite or monazite and also to the uncertainty in the blank correction, which made up as much as 10% of some LREE measurements. The blank for HF dissolutions was 0.2 ng for Nd. Examples of reproducibility and blank determinations are given in Walker (1984).

Analyses for U, Th, Ta, Cs, and Sr were obtained by instrumental neutron-activation analysis using the techniques described by Laul (1979). The reproducibility of these elements is better than 4%. Analyses for Nb, Rb, and Zr were obtained by energy-dispersive X-ray fluorescence with 3% reproducibility of Rb and 5% of Nb and Zr. The major-element determinations for perthite powders and whole-rock samples were also obtained using INAA and XRF. Li analyses were done by atomic absorption with an approximate analytical uncertainty of 5%.

Oxygen-isotope analyses were made by reacting approximately 15 mg of sample with ClF_3 in Ni reaction vessels heated to 550°C. The liberated oxygen was reacted with a carbon rod, heated to approximately 750°C, to produce CO_2 , which was subsequently analyzed using an isotope-ratio mass spectrometer. Reproducibility of analyses of all samples is typically within $\pm 0.05\%$ of the mean.

The F content of amblygonite-montebasite (LiAlPO_4F - $\text{LiAlPO}_4(\text{OH})$) was determined using the X-ray diffractometry techniques described by Černá et al. (1972). Major-element compositions of minerals were obtained using an automated ARL-EMX-SM electron microprobe. Data were reduced by the methods of Bence and Albee (1968) using the correction factors of Albee and Ray (1970).

GEOLOGY AND PETROLOGY

The Tin Mountain pegmatite is located in the Fourmile quadrangle of the southern Black Hills (Redden, 1963), cropping out approximately 12 km to the southwest of the main body of the Harney Peak Granite (Fig. 1). Riley (1970) reported a Rb-Sr whole-rock isochron age of 1.70 Ga for the granite, and the pegmatite is probably the same age. The pegmatite intrudes the early Proterozoic quartz-mica schist of the Mayo Formation and a small tabular unit of amphibolite. The intrusive contact is generally concordant with foliation in the schist. At the time of emplacement, the area was undergoing metamorphism near the first sillimanite isograd at an estimated pressure of 30 to 40 MPa (Redden et al., 1982).

The pegmatite crops out as an L-shaped body with a "lower leg" trending $\text{N}7^\circ\text{W}$, and an "upper leg" trending $\text{N}75^\circ\text{W}$ and plunging approximately 20° in that direction (Fig. 2). The upper leg is 90 m in length with a maximum width of 16 m and thickness of 30 m. The "lower leg" extends at least 100 m and has a maximum width of 25 m and thickness of 30 m.

Staatz et al. (1963) defined six major lithologic-structural zones in the pegmatite. Additional mapping of the internal structure of the body was conducted for the pur-

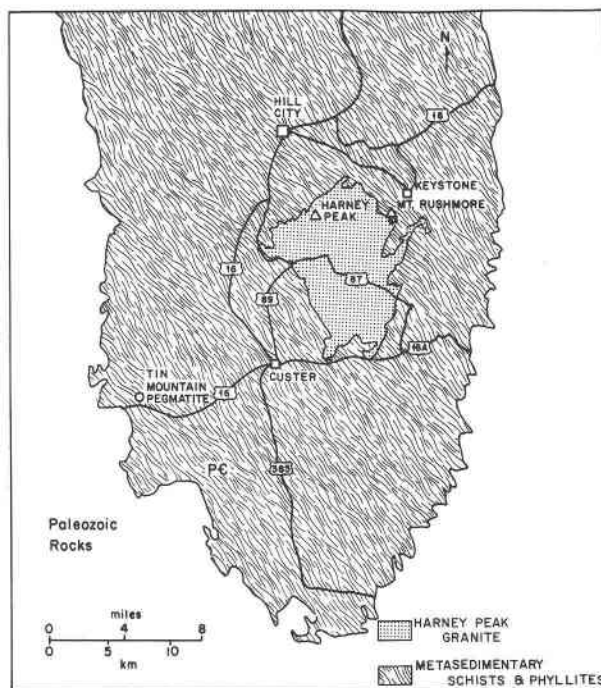


Fig. 1. Map showing the southern Black Hills, including the Tin Mountain pegmatite and the main outcrop of Harney Park Granite. (modified after Redden et al., 1982).

pose of this study during the summer of 1981. Mining, postdating the 1948 mapping published in Staatz et al. (1963), provided additional exposures, although the lower workings described in that study are inaccessible because of flooding.

Five zones are examined for this study: wall zone, first intermediate zone, second intermediate zone, third intermediate zone, and core (Fig. 2). The sixth zone defined by Staatz et al. (1963) is the border zone, a thin shell that surrounds the wall zone. Because of its volumetric insignificance, it was not examined.

Each zone is characterized by a distinct mineral assemblage. Significant modal variations are common within each zone, and the contacts between zones are generally gradational. The modal abundances of minerals within each zone were determined by the examination of drill cores in the study by Staatz et al. (1963), and are summarized in Table 1. Major-element compositions of each zone (Table 2) were calculated from the average modal mineralogy for each zone (normalized to weight percent) and the average mineral compositions, then normalized to 100%. From drill-core data and extensive mapping, we estimate that each of the five zones forms roughly 20% of the total volume of the pegmatite. The locations from which all samples were taken are detailed in Walker (1984).

Wall zone

The wall zone forms a concentric shell enclosing all other zones. It ranges in thickness from tens of centimeters to several meters. The zone is composed primarily of

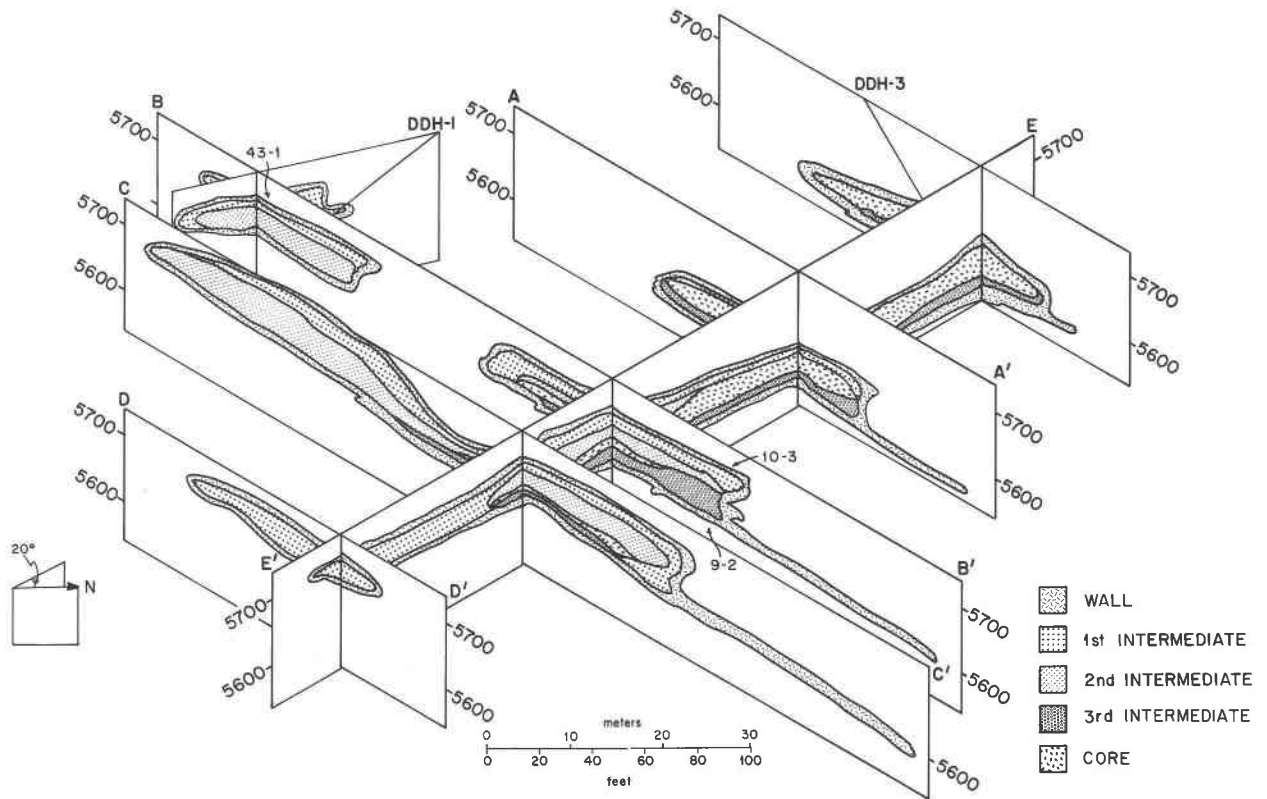


Fig. 2. Fence diagram and cross section of the Tin Mountain pegmatite showing the shape of the body and the relative positions of the five zones, constructed from updated cross-sectional diagrams of Staatz et al. (1963). The vertical scale gives feet above sea level and is reduced by $4 \times$ in the fence diagram. Section A-A' is shown with no vertical reduction for comparison. Approximate sampling locations for three wall zone samples are shown.

albite, quartz, and muscovite. The rock is equigranular and medium-grained to very coarse grained with crystals rarely exceeding 3 cm in maximum dimension.

Although the zone is modally inhomogeneous, the major-element compositions of the minerals vary little. Albite ranges from $Or_{1.4}Ab_{98}An_{0.6}$ to $Or_0Ab_{98.5}An_{1.5}$. However, FeO in muscovite ranges from trace amounts to 4.2 wt%. Major- and trace-element data, oxygen-isotope data,

and CIPW normative modes for three whole-rock samples of the wall zone are given in Table 3. The sampling locations for the three are shown in Figure 2. Small proportions of the wall zone have been albitized, probably the result of late-stage fluids. However, the consistency of albite compositions throughout the zone suggest that the majority of the zone was not recrystallized by late-stage fluids.

Table 1. Modal mineralogy (volume percent) of the five major zones of the Tin Mountain pegmatite, reported by Staatz et al. (1963)

Zone	WZ	1ST	2ND	3RD	Core
Quartz	34	33	7	27	55
Albite	54	10	2	43	6
K-Spar	tr	50	89	tr	tr
Mica	12	7	1	2	15
Spodumene	tr	tr	1	26	23
Amblygonite	tr	tr	tr	1	0.5
Beryl	tr	tr	tr	1	0.5

WZ-wall zone, 1ST-first intermediate zone, 2ND-second intermediate zone, 3RD-third intermediate zone, tr-trace.

First and second intermediate zones

First and second intermediate zones occur as tabular units found primarily in the upper parts of the pegmatite, particularly the upper leg. The first intermediate zone typically overlies and grades into the second intermediate zone. They reach maximum thicknesses of approximately 6 and 12 m, respectively, and pinch-out downward near the level of the core.

The first intermediate zone consists mainly of perthite, quartz, and albite, with minor muscovite. Perthite crystals are typically subhedral to euhedral with crystals extending up to 2 m in length. The exsolved, albite lamellae are as much as 2 mm thick. Quartz, albite, and muscovite occur in the much finer grained (millimeter- to centimeter-sized) matrix and are also found as inclusions within the perthite. These textural relations suggest that perthite and inclusions crystallized first, with interstitial minerals crystallizing subsequently. Bulk perthite crystals range from $Or_{70}Ab_{30}An_0$ to $Or_{75}Ab_{25}An_0$. K-feldspar compositions range from $Or_{94}Ab_6$ to $Or_{98}Ab_2$ and contain less than 0.1 wt% CaO and FeO. Exsolved albite is greater than $Ab_{99.5}$, whereas matrix albite ranges from $Or_{1.0}Ab_{99.0}An_0$ to $Or_{0.1}Ab_{99.7}An_{0.2}$.

The second intermediate zone is composed almost wholly of perthite crystals up to 4 m across. Quartz is a minor phase, occurring in the medium-grained matrix as inclusions within the perthite and as meter-sized anhedral crystals. Albite and muscovite are also found in the matrix.

The composition of the bulk perthite crystals ranges from $Or_{75}Ab_{25}An_0$ to $Or_{80}Ab_{20}An_0$; thus they are more potassic than perthite of the first intermediate zone. The

Table 2. The calculated chemical composition of each zone (weight percent) based on the weight-normalized mineral modes (Table 1) and average mineral compositions (compositions of zones normalized to 100%)

Zone	WZ	1ST	2ND	3RD	Core
SiO ₂	76.90	75.20	67.80	76.54	82.90
Al ₂ O ₃	15.40	14.70	18.30	16.40	13.00
Na ₂ O	6.30	3.30	2.77	4.89	0.88
K ₂ O	1.40	6.80	11.10	0.29	1.53
Li ₂ O	---	---	0.03	1.89	1.69

Table 3. Whole-rock compositions, isotopic data, and CIPW normative mineral modes for wall-zone samples

Sample #	9-2	10-3	43-1
(Wt. %)			
SiO ₂	74.40	68.32	70.78
TiO ₂	0.02	0.02	0.08
Al ₂ O ₃	13.54	17.54	15.67
FeO	2.20	1.54	0.51
MnO	0.05	0.26	0.05
MgO	0.02	0.01	0.01
CaO	0.64	0.93	0.61
Na ₂ O	2.68	9.13	8.01
K ₂ O	2.22	0.39	2.01
P ₂ O ₅	0.56	1.12	0.50
Sum	96.33	99.26	98.23
(ppm)			
Sr	23	74	50
Sr (c)*	(17)	(72)	(44)
Ba	71	70	60
Rb	890	253	910
Cs	183	190	183
Li	308	157	422
Ce	4.19	1.25	3.60
Nd	2.15	0.471	1.32
Sm	0.551	0.137	0.530
Eu	0.245	0.0106	0.0581
Gd	0.622	0.171	0.742
Dy	0.629	0.174	1.40
Er	0.248	0.0504	0.334
Yb	0.172	0.0376	0.282
δ ¹⁸ O _{SMOW}	12.1	11.3	11.7
CIPW Norms			
Quartz	47.42	12.09	15.22
Orthoclase	13.96	2.25	11.75
Albite	25.60	77.32	70.91
Corundum	8.02	3.30	0.44
Hypersthene	3.74	2.73	0.0
Magnetite	0.0	0.0	0.53
Ilmenite	0.03	0.02	0.11
Apatite	1.25	2.29	1.04

*Sr(c)=common Sr (total Sr-radiogenic Sr)

composition of exsolved albite is identical to that in perthite of the first intermediate zone. Matrix albite is generally $Or_{0.5}Ab_{99.4}An_{0.1}$.

Third intermediate zone

The third intermediate zone occurs primarily in the lowest parts of the pegmatite (Fig. 2). It pinches-out upward at the level of the core and grades into the second intermediate zone. The zone is a very coarse grained to pegmatitic equigranular rock composed of albite, quartz, spodumene, and mica. Subhedral crystals rarely exceed 5 cm. Within this matrix are spodumene laths 0.2 to 1 m in length. Apatite occurs as a trace phase both as small inclusions and centimeter-sized anhedral grains in the matrix. Albite is $Or_{0.5}Ab_{99.0}An_{0.1}$ to $Or_{0.2}Ab_{99.8}An_0$. Muscovite has typically 1 to 3 wt% FeO, which is, on the average, greater than in muscovite from other zones.

Core

The core is centrally located in the pegmatite, extending in the direction of the lower leg (Fig. 2). Only a small

Table 4. Compositional and isotopic data for mineral separates from the Tin Mountain pegmatite

Smp#	11-3A	11-3B	11-3C	11-4A	11-5A	11-6A	11-7A	13-3A	13-3B	13-3C	13-3E	13-4B	13-4C	13-4D
Min	Qtz	Musc	Plag	Ksp	Ksp	Ksp	Spod	Plag	Musc	Musc	Qtz	Qtz	Lepid	Plag
Zone	WZ	WZ	WZ	1ST	1ST	1ST	FF	3RD						
(Wt %)														
SiO ₂	---	45.93	68.65	64.8	65.2	64.3	65.55	68.28	45.65	45.08	---	---	---	69.27
Al ₂ O ₃	---	36.11	20.28	20.1	19.6	20.3	27.80	19.16	36.67	36.19	---	---	---	19.27
FeO	---	1.28	0.03	0.04	0.03	0.02	0.03	0.02	1.15	0.39	---	---	---	---
MnO	---	0.03	---	---	---	---	---	---	0.05	0.01	---	---	---	---
MgO	---	---	---	---	---	---	---	---	---	---	---	---	---	---
CaO	---	0.01	0.10	0.02	0.50	0.09	---	0.01	---	---	---	---	---	---
Na ₂ O	---	0.77	11.36	3.50	3.33	3.21	---	11.75	0.18	0.32	---	---	---	11.87
K ₂ O	---	10.01	0.06	11.29	11.50	12.35	---	0.06	10.71	10.42	---	---	---	0.41
Cr ₂ O ₃	---	---	---	---	---	---	---	---	---	---	---	---	---	---
P ₂ O ₅	---	---	---	---	---	---	---	---	---	---	---	---	---	---
Sum		94.14	100.48	99.75	100.16	100.27		99.28	93.41	92.45				100.82
(ppm)														
Sr	10.0	58.0	370	78.7	223	215	2.89	31.6	96.0	79.4	5.59	---	---	17.2
Rb	14.0	5870	51.4	4790	4940	6230	87.4	29.4	11600	11800	2.30	---	12100	428
Cs	14.5	530	16.4	---	---	---	---	9.18	---	1500	2.81	---	---	---
U	0.12	1.3	2.0	---	96	110	<5.5	2.4	18	<1.0	0.17	---	---	---
Th	---	---	0.065	---	---	---	---	0.069	---	---	---	---	---	---
Ta	1.5	78	1.5	---	---	---	---	9.1	---	160	0.68	---	---	---
Nb	---	300	---	---	<3.8	6.0	15	3.6	---	240	---	---	240	7.0
Zr	---	---	---	---	---	---	---	23	710	---	---	---	48	---
(ppb)														
Ce	---	302	195	77.4	16.4	289	37.9	414	---	386	---	---	111	1650
Nd	---	169	98.5	25.5	12.9	212	18.3	72.1	---	213	---	---	60.1	325
Sm	---	4.38	14.1	6.19	2.99	38.9	3.33	6.35	---	35.2	---	---	9.96	20.0
Eu	---	0.968	6.58	6.04	5.17	11.7	0.619	1.72	---	5.49	---	---	2.34	5.53
Gd	---	5.35	12.9	7.83	3.47	31.7	4.35	5.17	---	29.0	---	---	12.3	10.8
Dy	---	7.12	12.4	8.50	2.31	23.7	3.92	3.93	---	16.5	---	---	9.12	9.16
Er	---	2.24	6.07	2.89	1.34	9.80	2.07	1.97	---	7.42	---	---	4.10	3.23
Yb	---	2.08	5.30	2.55	0.791	7.89	1.76	1.52	---	5.71	---	---	3.07	2.73
δ ¹⁸ O _{SHOW}	12.4	10.0	11.0	11.3	11.2	11.4	10.2	11.0	---	10.3	12.6	12.7	10.0	11.6

Smp#	13-4E	15-1A	15-1B	15-1C	15-2	15-3A	15-3B	16-2A	16-2B	16-2C	16-2D	16-3A	16-3B	16-3C
Min	Musc	Qtz	Ksp	Spod	Xsp	Qtz	Spod	Amb	Musc	Qtz	Plag	Plag	Ksp	Qtz
Zone	3RD	FF	FF	FF	1ST	FF	FF	3RD	3RD	3RD	3RD	2ND	2ND	2ND
(Wt %)														
SiO ₂	45.70	---	64.8	---	65.3	---	---	---	47.04	---	68.38	69.79	67.8	---
Al ₂ O ₃	36.71	---	18.9	---	19.46	---	---	---	28.94	---	20.22	19.87	15.4	---
FeO	---	---	0.02	---	0.03	---	---	---	3.38	---	0.02	0.01	---	---
MnO	---	---	---	---	---	---	---	---	0.41	---	---	---	---	---
MgO	---	---	---	---	---	---	---	---	---	---	---	---	---	---
CaO	---	---	0.51	---	---	0.11	---	---	---	---	0.04	---	---	0.78
Na ₂ O	0.22	---	1.56	---	3.51	---	---	---	0.23	---	11.53	11.64	2.8	---
K ₂ O	11.04	---	13.7	---	11.53	---	---	---	10.05	---	0.05	0.09	12.8	---
Cr ₂ O ₃	---	---	---	---	---	---	---	---	---	---	---	---	---	---
P ₂ O ₅	---	---	---	---	---	---	---	---	---	---	---	---	---	---
Sum	93.70		99.59		99.94				90.15		100.24	101.40	99.58	
(ppm)														
Sr	46.5	---	86.8	<1.1	62.9	---	5.16	118	91.7	---	43.5	20	100	---
Rb	8140	1.48	8920	5.56	5510	---	5.38	17.4	11.4	13200	21.2	300	110	10000
Cs	---	3.32	312	9.06	---	---	2.59	11.7	7.49	460	7.27	88.8	25	1500
U	<41	0.0057	<0.78	0.032	---	<0.006	0.090	<0.5	<2.2	0.032	0.97	7.6	440	---
Th	---	---	---	---	---	---	---	---	---	---	0.060	---	---	---
Ta	---	0.042	0.45	0.59	---	0.11	1.2	160	230	0.52	4.9	---	---	---
Nb	240	---	<2.0	<1.3	2.0	---	---	<1.6	120	---	<1.6	<2	<5	---
Zr	<1.5	---	---	1.8	---	---	---	---	---	---	15	2.4	<2	---
(ppb)														
Ce	29.8	---	18.4	114	73.5	---	10.2	10.0	202	---	88.5	58.8	34.6	---
Nd	9.88	---	31.4	58.7	27.1	---	7.83	4.95	62.8	---	273	198	27.3	---
Sm	1.42	---	6.89	13.3	5.13	---	1.77	9.23	8.92	---	3.45	29.4	5.09	---
Eu	0.392	---	1.75	2.55	5.19	---	0.515	0.150	2.21	---	0.924	6.42	1.26	---
Gd	1.86	---	9.68	15.6	5.30	---	2.72	0.814	12.0	---	4.48	23.0	5.80	---
Dy	1.35	---	7.51	20.3	4.83	---	2.52	0.530	8.17	---	3.27	15.6	4.11	---
Er	0.028	---	5.12	14.7	1.53	---	1.99	0.257	5.10	---	2.08	7.63	2.34	---
Yb	0.950	---	3.81	14.1	1.01	---	1.67	0.182	4.04	---	1.65	5.83	1.79	---
δ ¹⁸ O _{SHOW}	10.2	12.6	11.4	11.8	11.4	12.8	10.4	11.7	9.8	12.9	11.4	10.9	11.4	12.8

portion of the core extends into the upper leg but is the dominant inner zone down dip in the lower leg.

The core is composed of quartz, spodumene, and mica with minor albite, beryl, and amblygonite. Quartz occurs as anhedral masses up to 1 m across. Spodumene forms euhedral to subhedral laths up to 5 m long. Both muscovite and Li-micas are found in the core. Muscovite occurs as millimeter-sized inclusions within quartz and spodumene and as platy books several centimeters in length. Muscovite has also a curvilamellar or "ball-peen" habit within the core. Li-micas, including lepidolite, occur as small aggregates sometimes intergrown with quartz,

frequently replacing spodumene. Albite is medium-grained cleavelandite (tabular habit), with masses rarely exceeding several centimeters across. Beryl crystals are as much as 1 m across. Amblygonite occurs as subhedral to anhedral masses with maximum dimensions greater than 1 m. Amblygonite also occurs as inclusions in quartz and micas. A large deposit of pollucite (Cs_{1-x}Na_xAlSi₂O₆·xH₂O) was reportedly mined from the upper core or second intermediate zone (W. Roberts, South Dakota School of Mines, pers. comm.).

Spodumene contains very little Fe and Mn (less than 1 wt% FeO and MnO combined). Albite ranges from

Table 4—Continued

Smp1#	16-5	16-6	16-7A	16-7B	16-8	16-9A	16-9B	16-10A	16-10B	16-10C	16-11A	16-11B	16-12A	16-12B
Min	Qtz	Spod	Musc	Qtz	Musc	Qtz	Plag	Qtz	Plag	Musc	Qtz	Plag	Plag	Qtz
Zone	Core	Core	Core	Core	2ND	3RD	3RD	3RD	3RD	3RD	3RD	3RD	Core	Core
(Wt %)														
SiO ₂	---	---	---	---	48.55	---	68.68	---	68.59	---	---	69.36	69.23	---
Al ₂ O ₃	---	---	---	---	34.33	---	20.18	---	20.05	---	---	19.48	19.61	---
FeO	---	---	---	---	1.33	---	0.01	---	0.01	---	---	---	0.01	---
MnO	---	---	---	---	0.15	---	---	---	---	---	---	---	---	---
MgO	---	---	---	---	---	---	---	---	---	---	---	---	---	---
CaO	---	---	---	---	0.05	---	0.07	---	---	---	---	---	---	---
Na ₂ O	---	---	---	---	0.05	---	11.79	---	11.90	---	---	12.03	11.73	---
K ₂ O	---	---	---	---	10.45	---	---	---	---	---	---	0.02	---	---
Cr ₂ O ₃	---	---	---	---	---	---	---	---	---	---	---	---	---	---
P ₂ O ₅	---	---	---	---	---	---	---	---	---	---	---	---	---	---
Sum					94.92		100.73		100.55			100.89	100.56	
(ppm)														
Sr	---	---	36.7	---	80.8	---	37.6	---	47.2	112	---	13.6	45	---
Rb	---	---	6180	---	11000	---	122	---	99.0	16500	19.7	125	180	---
Cs	---	---	---	---	---	---	---	---	---	---	6.12	61.8	33	---
U	---	---	90	---	<65	---	---	---	<6.3	---	0.28	1.0	10	---
Th	---	---	---	---	---	---	---	---	---	---	---	0.82	---	---
Ta	---	---	---	---	---	---	---	---	---	---	18	30	---	---
Nb	---	---	11	---	250	---	2.9	---	2.7	250	---	4.9	<2	---
Zr	---	---	---	---	<1.8	---	---	---	<1.3	<2	4.3	---	<2	---
(ppb)														
Ce	---	41.7	---	---	26.9	---	178	---	---	---	---	---	239	---
Nd	---	31.3	---	---	19.7	---	118	---	---	---	---	---	105	---
Sm	---	7.46	---	---	3.72	---	19.8	---	---	---	---	---	22.3	---
Eu	---	1.47	---	---	0.905	---	4.68	---	---	---	---	---	4.76	---
Gd	---	8.14	---	---	4.75	---	21.0	---	---	---	---	---	22.9	---
Dy	---	9.01	---	---	4.04	---	11.4	---	---	---	---	---	13.1	---
Er	---	3.73	---	---	2.36	---	4.34	---	---	---	---	---	5.25	---
Yb	---	3.21	---	---	2.02	---	2.71	---	---	---	---	---	2.91	---
$\delta^{18}\text{O}_{\text{SMOW}}$	12.6	10.5	10.8	13.2	10.5	12.5	11.5	12.5	11.2	9.9	12.6	11.4	11.0	12.6

Smp1#	16-13A	16-13B	16-14A	16-14B	17-1A	17-1B	17-1C	17-2A	17-2B	18-1A	18-1B	18-1C	18-1D	18-2A
Min	Qtz	Spod	Qtz	Plag	Ksp	Amb	Qtz	Ksp	Qtz	Musc	Qtz	Spod	Beryl	Qtz
Zone	Core	Core	3RD	3RD	2ND	2ND	2ND	2ND	2ND	Core	Core	Core	Core	Core
(Wt %)														
SiO ₂	---	---	---	69.29	64.5	---	---	64.9	---	46.36	---	65.67	---	---
Al ₂ O ₃	---	---	---	19.23	18.7	---	---	19.3	---	33.96	---	27.36	---	---
FeO	---	---	---	0.01	0.03	---	---	0.03	---	0.18	---	0.20	---	---
MnO	---	---	---	---	---	---	---	---	---	0.01	---	0.01	---	---
MgO	---	---	---	---	---	---	---	---	---	---	---	---	---	---
CaO	---	---	---	0.01	0.61	---	---	0.33	---	0.04	---	---	---	---
Na ₂ O	---	---	---	11.78	1.76	---	---	2.29	---	0.62	---	0.01	---	---
K ₂ O	---	---	---	0.02	13.0	---	---	12.3	---	9.92	---	---	---	---
Cr ₂ O ₃	---	---	---	---	---	---	---	---	---	---	---	---	---	---
P ₂ O ₅	---	---	---	---	---	---	---	---	---	---	---	---	---	---
Sum				100.34	98.6			99.20		91.09				
(ppm)														
Sr	---	---	---	20.0	82.7	577	4.32	82.7	---	64.2	---	1.46	---	---
Rb	---	---	---	120	8910	1.90	20.6	10400	---	10100	---	7.38	12.8	---
Cs	---	---	---	---	957	---	5.44	1070	---	8.94	1920	11.1	124	---
U	---	---	---	<6.3	<2.0	---	0.27	---	0.056	<0.9	0.063	<0.01	---	---
Th	---	---	---	---	0.28	---	8.2	0.36	0.65	100	2.3	0.94	---	---
Ta	---	---	---	---	---	---	---	---	---	---	---	---	---	---
Nb	---	---	---	<1.4	20	16	---	---	---	---	---	---	---	---
Zr	---	---	---	<1.2	39	---	---	---	---	---	---	---	---	---
(ppb)														
Ce	---	236	---	648	113	---	---	250	---	74.5	---	96.3	463	---
Nd	---	101	---	188	63.9	---	---	70.8	---	48.4	---	41.1	133	---
Sm	---	22.3	---	36.6	13.7	---	---	13.9	---	10.3	---	8.24	69.5	---
Eu	---	3.69	---	8.55	4.19	---	---	3.39	---	2.94	---	1.19	13.7	---
Gd	---	27.3	---	40.1	13.4	---	---	12.4	---	10.7	---	9.06	170	---
Dy	---	27.2	---	27.3	7.49	---	---	6.98	---	8.25	---	5.38	531	---
Er	---	10.2	---	11.1	2.68	---	---	2.66	---	4.33	---	1.98	288	---
Yb	---	8.29	---	5.72	1.47	---	---	1.43	---	3.38	---	1.71	770	---
$\delta^{18}\text{O}_{\text{SMOW}}$	13.2	10.5	12.5	11.2	11.4	11.5	12.5	11.8	12.7	---	12.7	10.4	---	12.7

Or_{0.3}Ab_{99.6}An_{0.1} to Or_{0.6}Ab_{99.4}An₀. In muscovite, FeO ranges from 0.2 to 3.0 wt%. Seven amblygonite samples have F contents ranging from 6.0 to 7.0 wt%; equal to approximately 50% amblygonite and 50% montebrasite.

Some secondary minerals and replacement textures are present in the upper part of the core. In many instances spodumene laths are rimmed with Li-mica, cookeite, cleavelandite, and lepidolite plus quartz. Green Li-micas also occur as a replacement of spodumene and quartz. London and Burt (1982) ascribe such mineral replacements to subsolidus cation exchange with late-stage fluids.

OXYGEN ISOTOPES

The $\delta^{18}\text{O}$ values of the whole-rock samples of wall zone range from 11.3 to 12.1‰ (Table 3). The isotopic data for mineral separates are given in Table 4. With few exceptions, the $\delta^{18}\text{O}$ values of all the major mineral phases sampled generally vary by less than 0.6‰: 12.4–12.9‰ for quartz, 11.0–11.6‰ for feldspars, and 9.9–10.2‰ for micas (Fig. 3). These $\delta^{18}\text{O}$ values are typical of unaltered granitoids (e.g., Taylor, 1968). However, the $\delta^{18}\text{O}$ values of spodumene vary much more widely from 10.2 to 11.8‰.

Table 4—Continued

Smp#	18-2B	18-2D	18-3A	18-3B	18-4A	18-4B	19-1A	19-1B	19-1C	20-1A	20-1B	20-1C	20-1D	22-1	22-6	31-1	32-1	33-1	35-1	43-1A
Min	Plag	Musc	Amb	Plag	Qtz	Amb	Qtz	Musc	Plag	Qtz	Ksp	Amb	Musc	Apt						
Zone	Core	Core	Core	Core	Core	Core	Core	Core	Core	2ND	2ND	2ND	2ND	2ND	3RD	Core	3RD	3RD	FF	WZ
(Wt %)																				
SiO ₂	68.40	46.97	---	69.24	---	---	---	45.00	68.60	---	67.0	---	49.59	---	---	---	---	---	---	---
Al ₂ O ₃	20.74	32.58	---	33.67	19.41	---	---	35.80	19.43	---	17.8	33.93	30.13	0.16	0.10	0.13	0.14	0.11	0.08	0.01
FeO	0.02	1.51	---	0.04	---	---	---	0.70	0.06	---	---	---	0.06	0.41	0.09	0.05	0.47	0.28	0.31	0.16
MnO	---	0.18	---	---	---	---	---	0.07	---	---	---	---	0.02	2.35	1.80	3.07	2.48	2.72	3.41	1.93
MgO	---	---	---	---	---	---	---	---	---	---	---	---	---	---	---	---	---	---	---	---
CaO	0.05	---	---	0.05	---	---	---	0.01	0.02	---	0.33	---	---	50.65	52.83	51.65	51.70	51.47	50.91	51.59
Na ₂ O	11.64	0.23	0.67	11.82	---	---	---	0.30	11.65	---	2.01	---	0.18	---	---	---	---	---	---	---
K ₂ O	0.14	10.28	---	0.07	---	---	---	10.70	0.11	---	12.1	---	11.02	---	---	---	---	---	---	---
Cr ₂ O ₃	---	---	---	---	---	---	---	---	---	---	---	---	---	---	---	---	---	---	---	---
P ₂ O ₅	---	---	---	---	---	---	---	---	---	---	---	---	---	---	---	---	---	---	---	---
Sum	100.99	91.75	---	100.63	---	---	---	92.58	99.87	---	99.24	---	91.00	95.89	96.75	97.55	97.36	97.07	96.96	---
(ppm)																				
Sr	22.7	---	130	44.9	---	---	2.27	59.3	29.3	---	71	---	---	310	131	---	144	131	2530	---
Rb	92.1	---	---	155	---	---	3.57	8310	601	---	7030	---	---	23.7	---	---	61.9	78.3	61.2	---
Cs	---	---	---	123	---	---	17.6	2500	---	---	930	---	---	---	---	---	---	---	---	---
U	---	---	1.9	0.35	---	---	---	---	---	---	440	---	---	---	---	---	---	---	---	---
Th	---	---	---	0.22	---	---	---	---	---	---	---	---	---	---	---	---	---	---	---	---
Ta	---	---	---	1.4	---	---	0.11	330	---	---	---	---	---	---	---	---	---	---	---	---
Nb	2.1	---	17	---	---	---	---	92	4.8	---	---	---	---	---	---	---	---	---	---	---
Zr	---	---	---	---	---	---	---	---	---	---	<5	---	---	---	---	---	---	---	---	---
	---	---	---	---	---	---	---	---	---	---	<2	---	---	---	---	---	---	---	---	---
(ppb)														(ppm)						
Ce	119	---	---	---	42.0	---	---	---	---	---	204	---	---	43.8	71.1	35.3	349	380	14.5	46.2
Nd	117	---	---	---	21.7	---	---	---	---	---	109	---	---	8.18	17.8	9.64	155	151	9.40	16.6
Sm	27.2	---	---	---	3.25	---	---	---	---	---	25.6	---	---	3.01	7.48	4.14	55.4	51.1	1.99	8.07
Eu	6.5	---	---	---	0.886	---	---	---	---	---	4.90	---	---	0.771	1.20	0.538	5.60	5.23	0.499	0.822
Gd	27.0	---	---	---	5.53	---	---	---	---	---	29.1	---	---	3.96	10.0	5.58	62.9	58.5	2.04	11.2
Dy	14.5	---	---	---	2.99	---	---	---	---	---	13.3	---	---	9.31	20.0	10.8	97.3	90.1	1.33	20.4
Er	5.95	---	---	---	1.74	---	---	---	---	---	3.61	---	---	3.16	5.85	2.09	32.3	32.7	0.599	4.73
Yb	3.82	---	---	---	1.01	---	---	---	---	---	1.49	---	---	5.40	7.87	1.60	27.8	29.0	0.407	3.62
$\delta^{18}O_{SMOW}$	11.2	9.9	11.6	11.3	12.4	10.9	12.5	10.0	11.3	13.1	11.3	11.3	10.0	9.3	9.4	9.1	9.5	9.5	8.9	10.5

TRACE ELEMENTS

Alkali and alkaline-earth elements

The trace-element compositions of all separated minerals are given in Table 4. The composition of the whole-rock samples of the wall zone are characterized by moderate Sr (23–74 ppm) and Ba (60–71 ppm), relatively high Rb (253–910 ppm), and very high Cs (183–190 ppm) and Li (157–422 ppm) concentrations, compared with average low-Ca granites (Turekian and Wedepohl, 1961). Common Sr contents (radiogenic ⁸⁷Sr subtracted, assuming crystallization approximately 1.70 Ga ago) range from 17–72 ppm (Table 3).

Rb concentrations in sampled perthite crystals from the first and second intermediate zones range from 4800 to 6200 ppm and 7030 to 10 000 ppm, respectively (Fig. 4). Perthite from the second intermediate zone also has highly variable Cs concentrations, ranging from 300 to 1000 ppm. The Sr contents of perthite from the first and second intermediate zones range from 60 to 220 ppm with two feldspars from the upper zone having the highest concentrations (Fig. 4). Common Sr contents range from 16 to 187 ppm. These results indicate that the Rb content of perthite generally increases toward the center of the pegmatite and common Sr content decreases. Shmakin (1979) and Černý et al. (1984) have also noted an increase of Rb and decrease of Sr in perthite toward pegmatite cores.

The Rb and Sr contents of albite from the core and third intermediate zones are highly variable and overlap substantially (Fig. 5). Albite from the wall zone (11-3C) has the highest Sr content of all sampled albite, and one of the lowest Rb contents. The Cs content of these albites varies from 9 to 125 ppm and generally correlates with Rb (Fig. 6).

The compositions of all muscovites from the core and second and third intermediate zones (no data exist for the first intermediate zone) overlap (Fig. 7). Muscovite from the wall zone (11-3B) has the highest common Sr content and lowest Rb content of all muscovite sampled.

Rare-earth elements

Whole-rock samples of the wall zone have widely variable REE patterns (Fig. 8). The pattern for whole-rock 43-1 mimics the shape of the pattern of apatite separated from the same rock. Wall zone 10-3 has a REE pattern similar to that of 43-1A. Whole-rock 9-2 has a positive Eu anomaly and a moderately LREE-enriched pattern.

Euhedral to anhedral apatites 1 to 4 cm in length were collected from throughout the pegmatite. All apatites are fluorapatites except for one hydroxyapatite (35-1), which was taken from a fracture filling (E. Foord, 1984, pers. comm.). The apatites have a large range of REE concentrations and a variety of patterns on chondrite-normalized plots. All apatite patterns except for the pattern of the hydroxyapatite are characterized by depletions in Nd relative to Ce and Sm, enrichments in Dy relative to Gd and Er, and by large negative Eu anomalies (Fig. 9). These REE patterns are unusual because REE's generally partition into minerals as a coherent group, with smooth chondrite-normalized patterns resulting (Hanson, 1980). Although "kinked" patterns such as these are rare, similar patterns have been noted in an albitized granite plug by Harris and Marriner (1980), in pegmatitic granites by Goad and Černý (1981) in tin granites by Chatterjee and Strong (1984), in fluorites by Strong et al. (1984), and in sapphirine granulites by Windrim et al. (1984). Although it has been shown that radiogenic Sr from adjoining phases

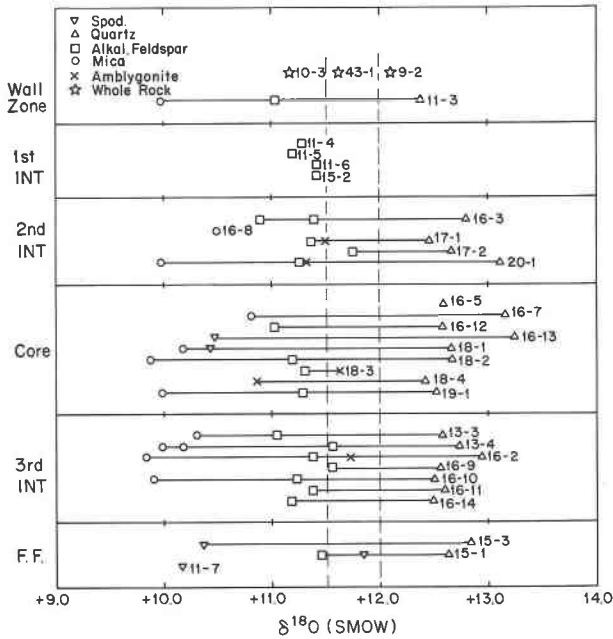


Fig. 3. Oxygen-isotope data for mineral separates and whole-rocks from the major zones of the Tin Mountain pegmatite and fracture fillings (FF).

has been incorporated into the apatites after crystallization (Riley, 1970; Walker, 1984), the REE patterns are probably not the result of alteration. The concentration of REE in the apatites is 10 to 1000 times greater than in adjoining phases, so that exchange was unlikely. It is possible that intergrowths of other phases such as allanite or monazite could cause the enrichment of Ce relative to Nd; however, no intergrowths have been detected. Because of the correlation between the kinking of REE patterns and

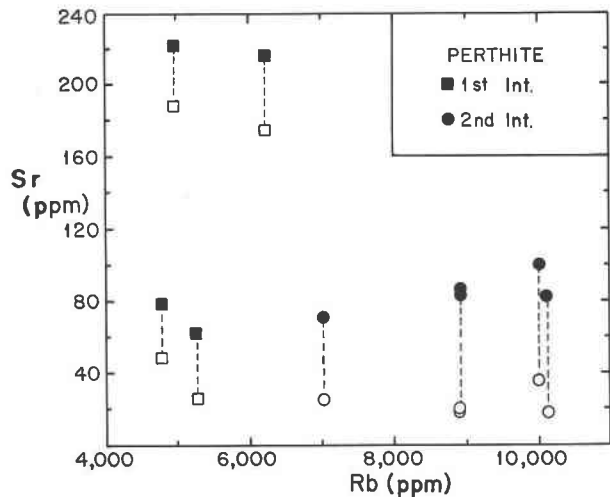


Fig. 4. Plot of Rb vs. Sr (solid symbols) for perthite separates from the first and second intermediate zones. Calculated common Sr concentrations (total Sr minus radiogenic Sr, assuming a 1.70 Ga crystallization age) are shown as open symbols.

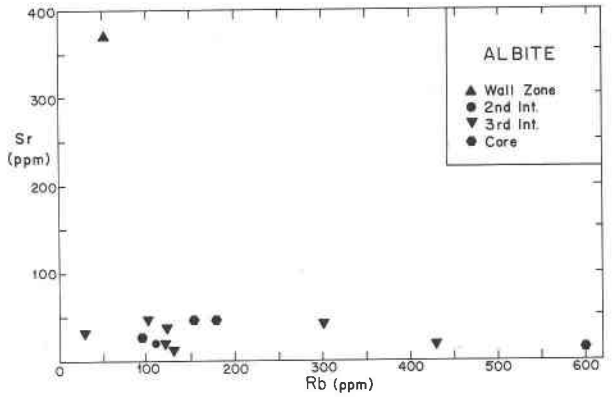


Fig. 5. Plot of Rb vs. Sr for albite separates. Plot shows the compositional overlap between the core, second and third intermediate zones. One sample from the wall zone has a very high concentration of Sr.

halogen- and fluid-rich systems, it is likely that the cause of kinking is the formation of REE-specific F, Cl, or P complexes (Mineyev, 1963) in an aqueous or carbonate fluid coexisting with the apatite and melt.

Representative REE patterns for a variety of pegmatite minerals from all zones are presented in Figure 10. The patterns for alkali feldspars from each of the zones are presented in Figure 11. Four characteristics are noted: (1) Only feldspars from the wall zone and first intermediate zone have positive Eu anomalies on chondrite-normalized patterns. (2) The Eu anomalies of minerals from the second and third intermediate zone and core (Fig. 12), such as micas and spodumene, mimic the anomalies in coexisting feldspars. Minerals from sample 16-2 in the third intermediate zone have similarly shaped patterns for muscovite, albite, and amblygonite with greater than one order of magnitude differences in concentrations. (3) In some instances, suites of minerals taken from the same sampling

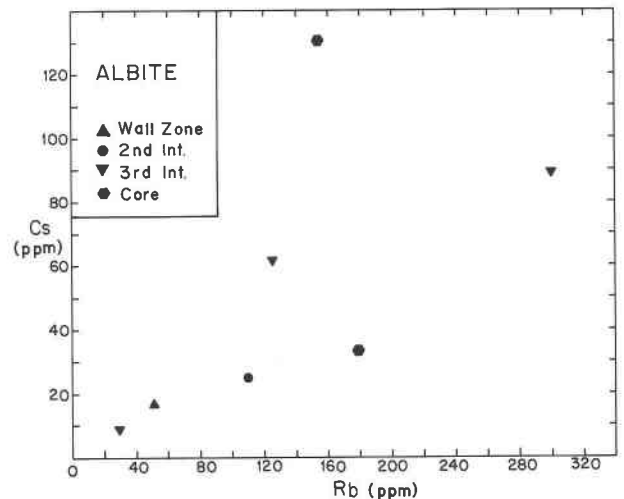


Fig. 6. Plot of Rb vs. Cs for albite separates. The trace alkalis show a positive correlation.

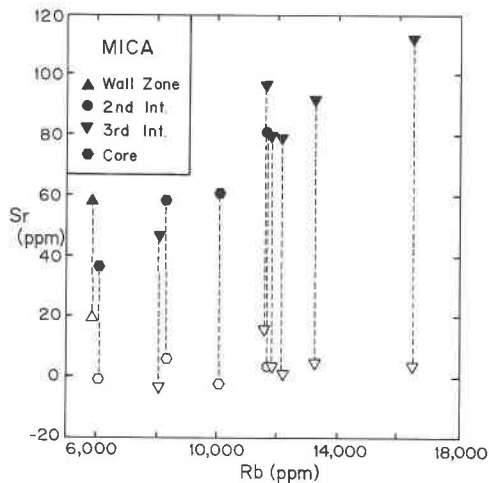


Fig. 7. Plot of Rb vs. total Sr (solid symbols) for mica. Calculated common Sr concentrations are shown as open symbols. Negative common Sr concentrations may reflect the analytical uncertainty or the mobility of Sr after crystallization.

station have a large diversity of pattern shapes (Figs. 11, 12, 13). Some suites, such as 16-3 (Fig. 11), have two distinct alkali feldspar patterns with very different $\delta^{18}\text{O}$ values of 10.9 and 11.4‰ (Table 4), indicating that the albite was likely formed as a secondary mineral, perhaps subsolidus. (4) All of the major phases have very low REE concentrations. Much higher REE concentrations are found in the trace phases apatite and to a lesser degree columbite-tantalite.

U and Th

The U/Th ratios of minerals from throughout the pegmatite are consistently large (Table 4), ranging from 1.2 to 34, compared with commonly reported granitoid ratios of 0.2 to 0.3 (Coates, 1956; Rogers, 1964; Hildreth, 1977). These ratios are similar to those of whole-rock samples of pegmatitic portions of the Harney Peak Granite (Walker, 1984). Large U/Th ratios may suggest that Th-rich phases crystallized at some stage of fractionation preceding the crystallization of the pegmatite. Also, under oxidizing conditions, U can form complexes that are soluble in aqueous and carbonate fluids (Rogers and Adams, 1969; DeVoto, 1978), possibly indicating that some phases crystallized from a U-rich fluid.

DISCUSSION

The lithologic, textural, and major-element compositional variations observed in the Tin Mountain pegmatite are similar to those noted in many other lithium-bearing zoned pegmatites throughout the world (e.g., Cameron et al., 1949; Norton et al., 1962; Norton, 1983).

Numerous models have been proposed for the crystallization of layered and zoned granitic pegmatites (Statz et al., 1955; Norton et al., 1962; Jahns and Burnham, 1969; Uebel, 1977; Stewart, 1978; Jahns, 1982; Norton, 1983). Most of these models require the initial crystalli-

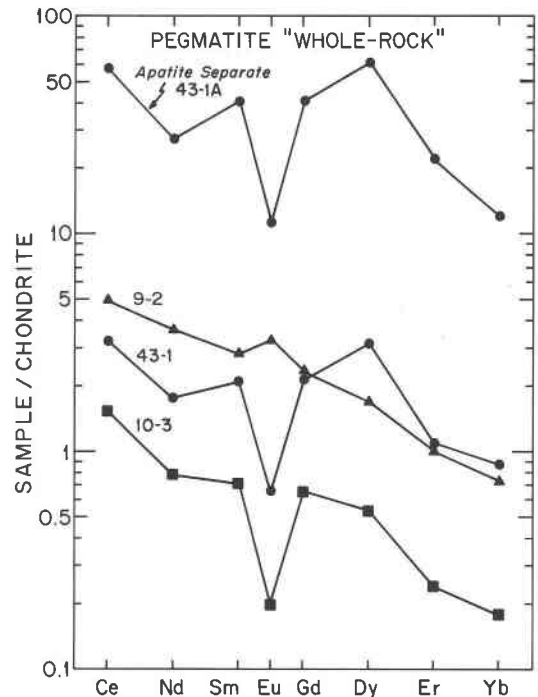


Fig. 8. Chondrite-normalized REE patterns of whole-rock samples of wall zone. The REE pattern of apatite separate 43-1A, also shown, is identical in shape to wall zone sample 43-1 from which it was taken, suggesting that the zone formed as an accumulation of crystals on the walls of the magma chamber.

zation of a wall zone, which encloses the remaining melt and provides a nearly closed system in which crystallization proceeds. Late-stage fracturing may breach the body, as indicated by fracture fillings that can be traced from some pegmatites into country rock. The results of previous studies have generally suggested that zoned pegmatites intruded as silicate melts, which exsolved aqueous fluids during some stage of crystallization, and that some late-stage assemblages result from crystallization solely from aqueous fluids. Results of a Sm-Nd isotopic study of the Tin Mountain pegmatite (Walker, 1984) suggest that mixing occurred between the REE of the pegmatite and the country rocks during crystallization and that the pegmatite was not a completely closed system at any time during its crystallization.

In order to determine the processes that resulted in the crystallization of the texturally and lithologically diverse Tin Mountain pegmatite, both geothermometry and trace-element concentrations are utilized to discern the order in which the different units crystallized.

Both geothermometers and trace-element trends are prone to subsolidus alteration and metamorphic disturbance. Care was taken to avoid sampling metasomatized portions of the pegmatite. No metamorphic recrystallization is evident in the Harney Peak Granite or pegmatites. However, the postcrystallization mobilization of radiogenic ^{87}Sr within the Harney Peak Granite and many of the pegmatites in the Black Hills is indicated by very

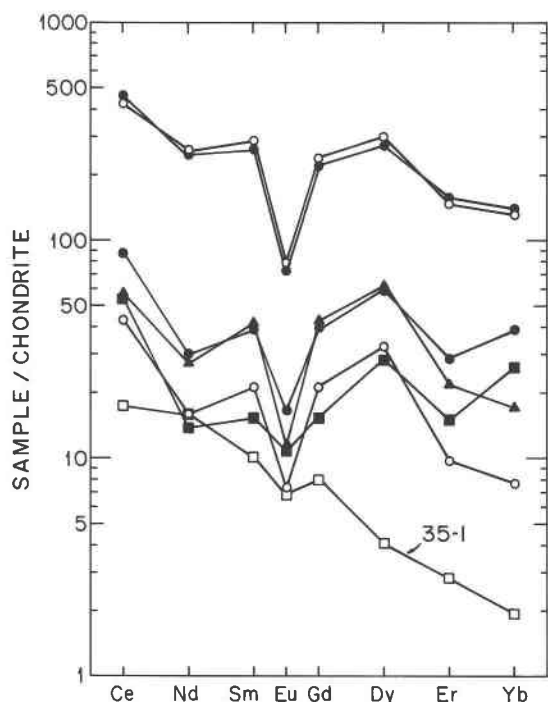


Fig. 9. Chondrite-normalized REE patterns of apatite. The kinked patterns may reflect REE-specific complexes forming within the melt or fluid from which they crystallized. Sample 35-1 is discussed in the text.

high concentrations of radiogenic Sr in phases with low Rb concentrations (Riley, 1970; Walker, 1984). Some of the anomalous $\delta^{18}\text{O}$ values (e.g., sample 16-3A) may reflect either subsolidus recrystallization or metamorphic re-equilibration.

While some movement of Sr evidently did occur after crystallization, the data suggest that most of the exchange of Sr occurred between micas and phosphates. Sr isotopic data for feldspars from pegmatites, including Tin Mountain (Riley, 1970), suggest that feldspars have retained most of their radiogenic ^{87}Sr and, consequently, their common Sr. There is no evidence to suggest that Rb was mobile after crystallization. Therefore, the trace-element trends of Rb and Sr as recorded in feldspars are probably the most useful for discerning the crystallization sequence of the pegmatite.

Geothermometry

Few currently calibrated geothermometers are viable in pegmatite systems and, in the case of the Tin Mountain pegmatite, only oxygen-isotope and two-feldspar geothermometers are even potentially applicable. Both are relatively imprecise and may be affected by subsolidus exchange.

The two-feldspar geothermometer of Whitney and Stormer (1977) yields crystallization temperatures of 650 to 600°C for several first-intermediate-zone feldspar pairs (samples 11-4, 11-5, 11-6, 15-2), and temperatures rang-

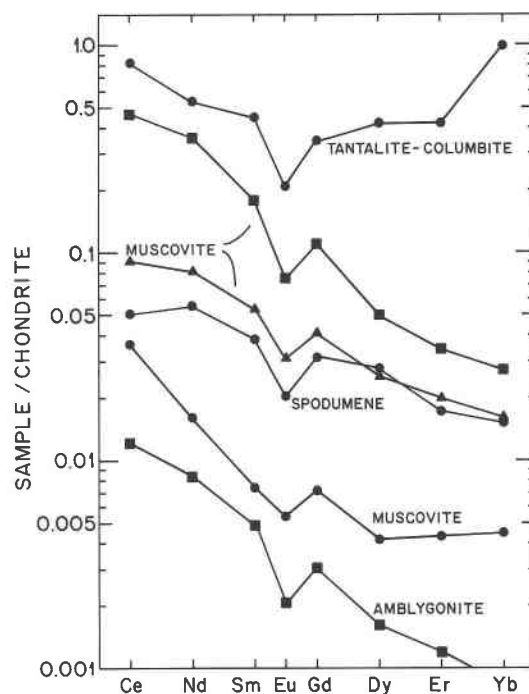


Fig. 10. Representative chondrite-normalized REE patterns of various pegmatite minerals. Large variations in concentrations, and low overall REE abundances are illustrated.

ing from 600 to 550°C for feldspar pairs from the second intermediate zone (samples 16-3, 17-1, 17-2, 20-1). These temperatures are at best relative, not absolute temperatures. The condition of equilibrium crystallization cannot be tested in these pairs, and Brown and Parsons (1981) have reported that problems of metastable crystallization may limit the quantitative use of two-feldspar geothermometry.

The application of oxygen-isotope geothermometry to the Tin Mountain pegmatite requires the retention of isotopic equilibrium after crystallization. The oxygen-isotope compositions of other pegmatite mineral assemblages have been examined in several studies, including those of Taylor et al. (1979), Longstaffe et al. (1981) and Taylor and Friedrichsen (1983b). These studies have shown that oxygen-isotope equilibrium is sometimes maintained in pegmatites. Taylor and Friedrichsen (1983a) discussed the problem of subsolidus exchange of oxygen in pegmatite systems. They suggested that the retention of isotopic zonation and crystal size indicate that accurate oxygen-isotope temperatures may be obtained from some pegmatite assemblages. The accuracy of temperatures determined by oxygen-isotope geothermometry is limited by the discrepancies of reported isotopic fractionations and by the uncertainty in the determination of the fractionations at low temperatures.

Eight temperature determinations using three-phase quartz-feldspar-muscovite assemblages and fifteen using two-phase quartz-muscovite and quartz-feldspar assemblages were made for the Tin Mountain assemblages based

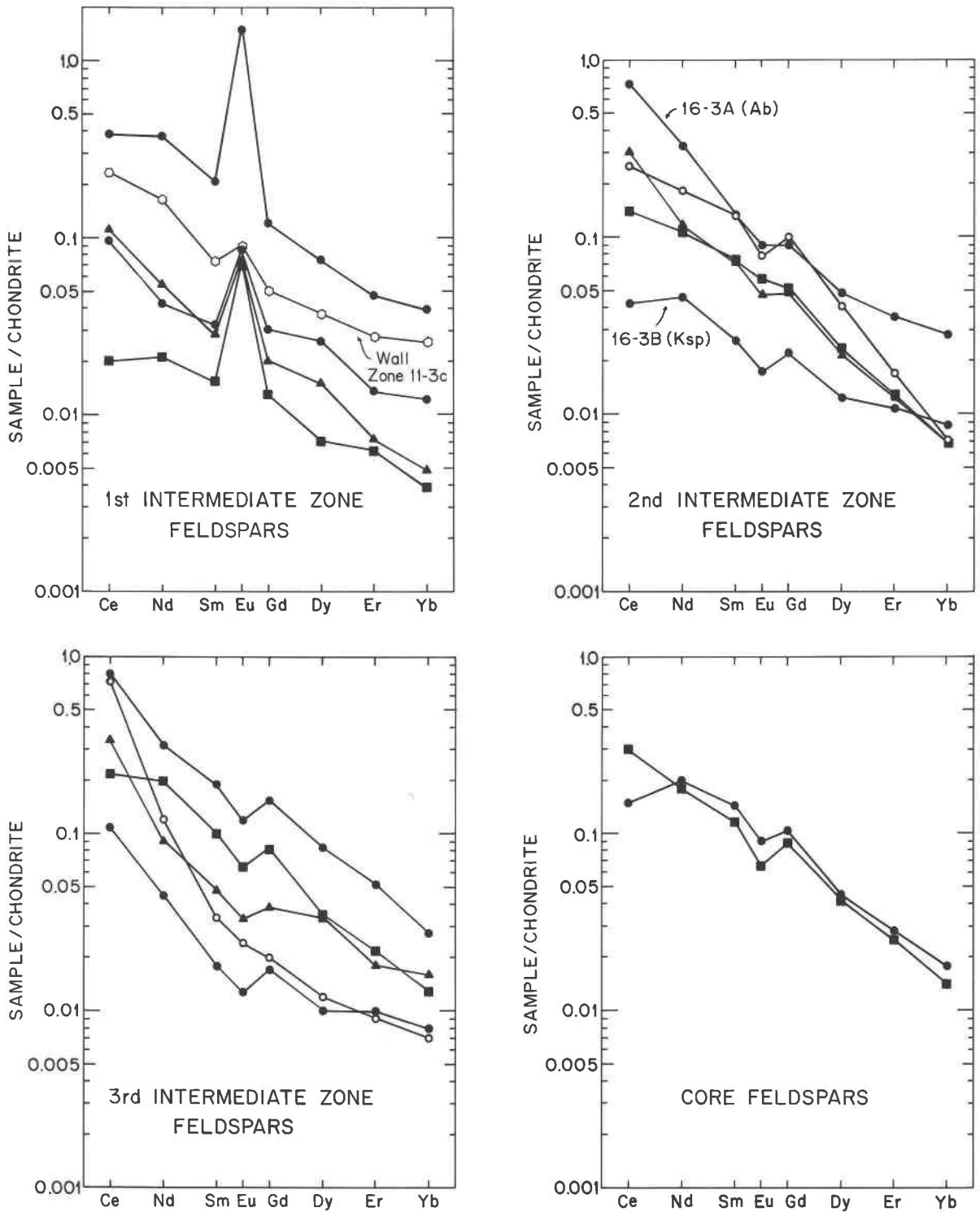


Fig. 11. Chondrite-normalized REE patterns of alkali feldspar samples from the wall zone and four inner zones. The positive Eu anomalies of K-feldspars from the first intermediate zone contrast with the absence of, or even negative anomalies present in, feldspars from the other inner zones.

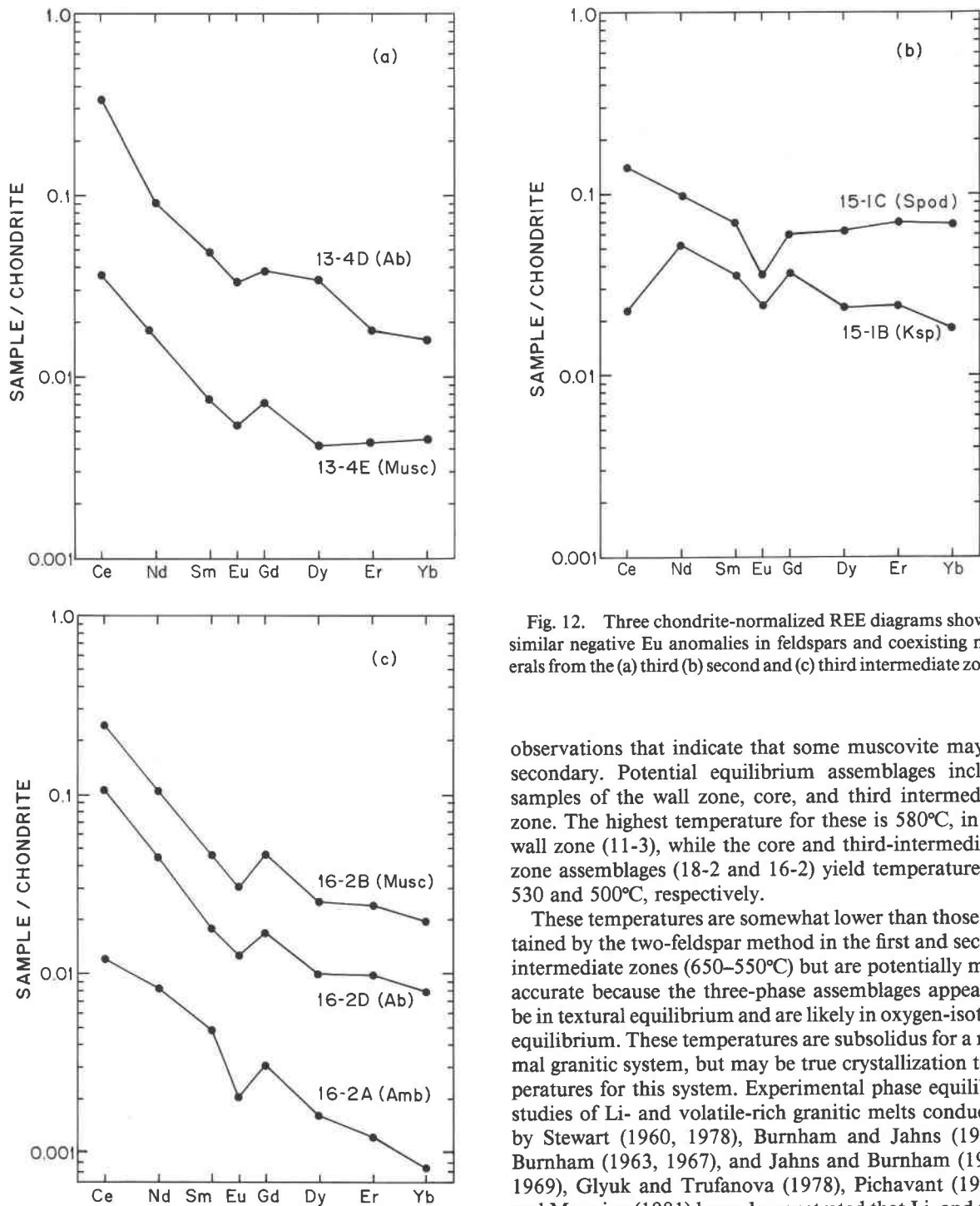


Fig. 12. Three chondrite-normalized REE diagrams showing similar negative Eu anomalies in feldspars and coexisting minerals from the (a) third (b) second and (c) third intermediate zones.

observations that indicate that some muscovite may be secondary. Potential equilibrium assemblages include samples of the wall zone, core, and third intermediate zone. The highest temperature for these is 580°C, in the wall zone (11-3), while the core and third-intermediate-zone assemblages (18-2 and 16-2) yield temperatures of 530 and 500°C, respectively.

These temperatures are somewhat lower than those obtained by the two-feldspar method in the first and second intermediate zones (650–550°C) but are potentially more accurate because the three-phase assemblages appear to be in textural equilibrium and are likely in oxygen-isotope equilibrium. These temperatures are subsolidus for a normal granitic system, but may be true crystallization temperatures for this system. Experimental phase equilibria studies of Li- and volatile-rich granitic melts conducted by Stewart (1960, 1978), Burnham and Jahns (1962), Burnham (1963, 1967), and Jahns and Burnham (1957, 1969), Glyuk and Trufanova (1978), Pichavant (1981), and Manning (1981) have demonstrated that Li, and volatiles such as F, Cl, B, and H₂O can significantly reduce liquidus and solidus temperatures of granitic melts and can alter the composition of the minimum melt in the Qz-Or-Ab system. Very high concentrations of Rb and Cs may further reduce solidus temperatures. As with two-feldspar geothermometry, however, the cooling trends indicated by the temperature determinations are emphasized rather than the absolute temperatures.

on the fractionation factors of Bottinga and Javoy (1975) (Fig. 14). The total range of isotopic temperatures determined using both two-phase and three-phase assemblages is 450 to 610°C. Of the eight three-phase assemblages, only three sets may be in isotopic equilibrium. In four of the five assemblages that are not in equilibrium, muscovite has anomalous $\delta^{18}\text{O}$ values, confirming petrographic

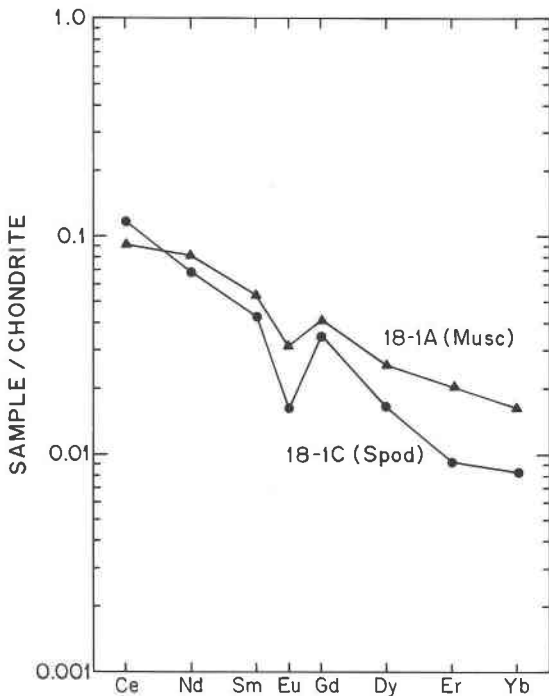


Fig. 13. Chondrite-normalized REE patterns of coexisting minerals from the core.

Trace-element trends

Some trace elements, particularly alkali and alkaline-earth elements, are potentially useful in discerning fractionation trends of granitic systems, including the internal evolution of pegmatites. Owing to the large grain size, obtaining compositionally representative whole-rock samples of a bulk pegmatite or even most zones was impossible. However, the trace-element composition of separated minerals may record the trace-element composition of the melt or fluid from which the minerals crystallized. This composition can be estimated using known mineral/melt or mineral/fluid distribution coefficients. Rb, Cs, Sr, and Ba are predominately concentrated within feldspars and micas in the Tin Mountain pegmatite. The behavior of these elements during a specified crystallization sequence can be modeled using published mineral/melt and mineral/fluid partition coefficients and modal abundances, assuming that they have not been affected by metamorphism.

As has been shown in other studies of granite systems (e.g., Hudson and Arth, 1983), crystal fractionation involving albite and K-feldspar should generally enrich residual silicate melt in more incompatible elements such as Rb and Cs and deplete the melt in compatible elements such as Sr and Ba. Distribution coefficients (K_d) for Rb, Cs, Sr, and Ba between feldspars and both granitic melt and aqueous fluids have been characterized by a number of studies (Arth, 1976; Carron and Lagache, 1980; Volfing and Robert, 1980). The partitioning characteristics of these elements between muscovite and a granitic melt

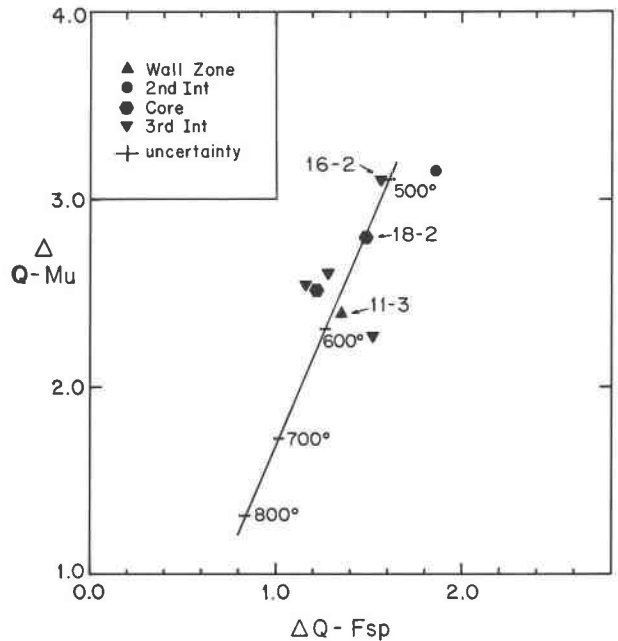


Fig. 14. $\Delta^{18}\text{O}$ quartz-muscovite and $\Delta^{18}\text{O}$ quartz-feldspar plot for quartz-muscovite-alkali feldspar assemblages from the Tin Mountain pegmatite. Crystallization temperatures of 580, 530, and 500°C are obtained for the three assemblages plotting on the equilibrium curve of Bottinga and Javoy (1975). The five other assemblages indicate disequilibrium crystallization or secondary exchange of oxygen isotopes.

are less well constrained, but estimates of their behavior are made using available biotite mineral-melt partitioning data, the aqueous fluid/muscovite data of Volfing and Robert (1980), and the coexisting biotite-muscovite trace-element data of Papike et al. (1983). Rhyolitic mineral/melt distribution coefficients for all subsequent modeling are taken from the compilation by Arth (1976) (see Table 5), except where noted.

Factors complicating the use of these K_d values include both the problem that all K_d values reported to date are for conditions under which feldspars are hypersolvus, unlike the subsolvus conditions under which Tin Mountain feldspars crystallized, and the uncertain effect volatiles have on K_d values. Although the absolute distribution coefficients for this system remain uncertain, it is likely that the relative differences between K_d values of the same element for different phases are similar to those in known systems.

Results from previous studies suggest that most parts of zoned pegmatites crystallize from coexisting aqueous fluid and silicate melt. As long as equilibrium is maintained between the two liquid phases and crystallizing minerals and the relative proportions of each liquid remain constant, the fractionation trend recorded by trace elements in crystalline material should be similar to trends recorded by crystallization from a single liquid. The behavior of these trace elements once all the melt was depleted and only fluid crystallization occurred would prob-

ably have been similar to their behavior during crystallization from both melt and coexisting fluid (Carron and Lagache, 1980; Volfinger and Robert, 1980). Therefore, we believe that granitic distribution coefficients should be useful for determining qualitative fractionation trends within pegmatites.

Other elements, such as REE, Ta, Nb, U, and Th, might also be incompatible in the crystallizing phases and concentrated in residual melt, although trace phases might control the behavior of these elements instead, as has been shown for the REE in granites (Miller and Mittlefehldt, 1982; Gromet and Silver, 1983). During crystallization of the Tin Mountain pegmatite, the concentration of REE was probably controlled by the crystallization of apatite, a phase with large mineral-melt K_d values. Apatite is unusually abundant in the pegmatite, in some parts exceeding 1% of the mineral mode. The trace phases columbite-tantalite and microlite controlled the behavior of Ta and Nb during crystallization. Therefore, the behavior of REE, Ta and Nb is difficult to model, given the poor determinations of the modal abundances of these phases. Except for apatite, no other U- or Th-rich phases have been found within the pegmatite, so these elements might have behaved more incompatibly throughout the crystallization sequence. However, no enrichment trends are observed in the data.

Composition of initial melt

The low Rb, Cs, and Li wall-zone concentrations and high Sr and Ba concentrations, relative to the rest of the body suggest that the wall zone was the first material to crystallize from the pegmatite melt. Wall-zone minerals albite 11-3C and muscovite 11-3B have the highest Sr concentrations and among the lowest Rb concentrations for these minerals within the pegmatite. The positive Eu anomaly in whole-rock wall-zone sample 9-2 reflects the REE pattern of feldspar, and the kinked REE patterns of wall-zone samples 10-3 and 43-1 reflect the patterns of apatite (Fig. 8). The REE pattern of 9-2 is consistent with the wall zone crystallizing first, but not from residual melt or fluid, and may indicate that the wall zone was isolated from later mineral-melt or mineral-fluid interaction. If parts of the wall zone crystallized from residual melt or fluid, the REE pattern of the rock would acquire the pattern of that melt or fluid and not have a positive Eu anomaly. Wall-zone samples 10-3 and 43-1 were collected from the headwall of the pegmatite (Fig. 2), a part of pegmatites that frequently shows metasomatic alteration, and their REE patterns may reflect either crystal accumulation or some metasomatic alteration.

If the composition of the wall zone was not modified by reaction with residual melt or fluids, the trace-element compositions of the three, whole-rock samples of wall zone can be used to constrain the composition of the intruding pegmatite melt. The best-fit, parent-melt compositions were determined for each whole-rock sample of wall zone. The parent-melt composition for each sample is the composition of melt that would fractionally crys-

Table 5. Mineral/melt partition coefficients used in calculations

Mineral	Albite	Or ₇₅	Musc
Rb	0.050	0.66	1.5*
Cs	(0.005)	(0.036)	1.5*
Sr	2.8	3.9	0.4*
Ba	0.36	6.1	12*
Li	0.02*	0.01*	0.5*

K_d 's taken from Arth (1976) and Carron and Lagache (1980) (), except where noted by *.

* Albite: Li-estimated from Shearer et al. (1984).

K-spar: Li-estimated from average Li K-spar data from Shearer et al. (1984) assuming crystallization from a Li saturated melt (6000 ppm).

Musc: Li, Rb, Sr, and Ba estimated from biotite K_d 's (Arth, 1976), combined with biotite/muscovite K_d 's determined by Papike et al. (1983) of 4, 2, 0.3, and 0.5 respectively. Cs-assumed similar to Rb.

Spodumene and quartz assumed to be 0.0 based upon the low concentrations of these elements within Tin Mountain quartz and spodumene.

tallize to produce a rock with the composition of the whole-rock samples. The modeling assumes that the wall zone composes about 20% of the volume of the pegmatite and that the bulk compositions represented by the CIPW normative modes of each sample of wall zone (Table 3) fractionally crystallized to produce each rock.

The compositions obtained for the three samples indicate that the parent melt had 3600–7000 ppm Rb, 680–3000 ppm Cs, 4000–10 000 ppm Li, 18–40 ppm Sr, and 40–84 ppm Ba (Table 6). The large range of compositions may reflect both different stages in the crystallization of the wall zone and possibly metasomatic alteration of 10-3 and 43-1. The concentrations of Rb and Li in minerals from throughout the pegmatite are more consistent with the lower estimates for these trace alkalis, and we estimate that the concentrations of Rb, Cs, Li, Sr, and Ba in the original melt were approximately 4000, 1000, 4000, 40, and 60 ppm respectively. While the modeling does not tightly constrain the concentrations of these elements in the parent melt, the ranges are useful in determining the derivation of the melt (Walker, 1984; Walker et al., 1985) and to use as an initial composition for modeling the internal evolution of the pegmatite.

Sequence of crystallization

The first intermediate zone crystallized following the crystallization of the wall zone. Crystallization of the first intermediate zone before the remaining inner zones is indicated both by the cooling trend from the first intermediate zone to the second intermediate zone, determined by two-feldspar geothermometry, and by the abrupt disappearance of positive Eu anomalies in feldspars between the first intermediate zone and the remaining inner zones (Fig. 11). The absence of positive Eu anomalies in feldspars from the core and from the third and second intermediate zones did not result from crystallization of earlier feldspar causing a depletion of Eu in the melt. Micas and spodumene have Eu anomalies similar to those of coexisting feldspars (Fig. 12). Eu depletion in the melt would be evidenced by very large negative Eu anomalies in the

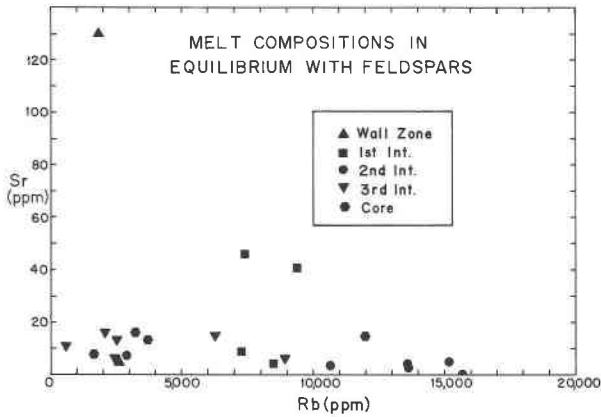


Fig. 15. Calculated Rb and Sr melt compositions coexisting with the feldspars, using K_d values from Arth (1976) and data in Table 4 (common Sr for K-feldspar).

micas and spodumene coexisting with the feldspars. Therefore, the negative anomalies in the feldspars may reflect the presence of predominately trivalent Eu in the melt or fluid from which they crystallized. The possible change of Eu from divalent to trivalent during the crystallization of the pegmatite may be attributed to one of at least two processes: (1) alteration of the structure of the melt to favor trivalent Eu, and (2) the increase of f_{O_2} in the melt to a level at which Eu is completely trivalent.

Möller and Muecke (1984) reviewed the effects of melt structure on the valence state of Eu. Their compilation of previous work indicates that the aluminum content of a melt might control the valence state of Eu at constant f_{O_2} by forming aluminosilicate complexes that preferentially stabilize Eu^{2+} relative to Eu^{3+} . Too little is known about this effect at present to assess whether a change in melt structure affected the valence of Eu in the Tin Mountain pegmatite.

Drake and Weill (1975) discussed the effect of f_{O_2} on the oxidation state of Eu. They found that at temperatures of 1000 to 1200°C, Eu^{3+} predominates near the hematite-magnetite buffer. If these results can be extrapolated to much lower temperatures, a predominance of Eu^{3+} in the pegmatite melt would require that the f_{O_2} of the system reached the magnetite-hematite buffer after the crystallization of the first intermediate zone. Such high f_{O_2} conditions have been determined by the examination of the oxidation state of Fe in biotites from the Harney Peak Granite (Shearer et al., 1984). The disappearance of positive Eu anomalies—whether the result of a change in the structure of the melt or in f_{O_2} —combined with other trace-element data indicates that crystallization proceeded from the first intermediate zone to the remaining inner zones.

The concentrations of Rb and Sr in the melt assumed to have coexisted simultaneously with feldspars in the core and in the second and third intermediate zones were calculated using mineral/melt distribution coefficients (Fig. 15). Considerable overlap between the concentrations of Rb and Sr is noted, suggesting simultaneous growth of

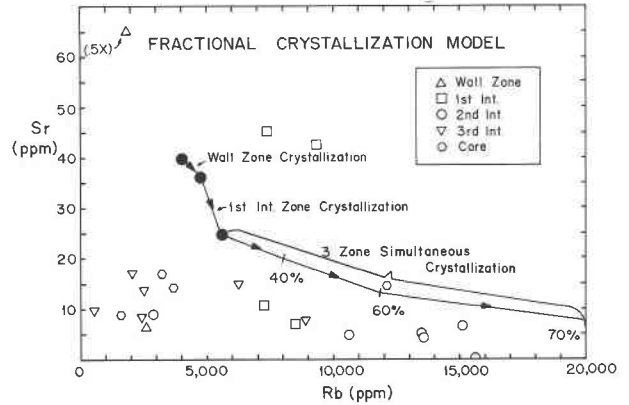


Fig. 16. Rayleigh fractionation model of the behavior of Sr and Rb during the sequential, then simultaneous crystallization of the Tin Mountain pegmatite. The crystallization path is (1) wall zone, (2) first intermediate zone, (3) then second and third intermediate zones and core. The bulk distribution coefficients for Rb for each path segment are 0.21, 0.44, and 0.30, respectively. Bulk distribution coefficients for Sr are 1.6, 2.3, and 1.7, respectively.

these zones. The REE patterns of the mineral separates from these zones are also consistent with the simultaneous, inward crystallization of the second and third intermediate zones and the core. The two oxygen-isotope temperatures for the core and third intermediate zone are lower than the temperature for the wall zone.

REE abundance vary considerably within each zone, probably resulting from the changing fractions of residual melt and fluid and from the crystallization of the trace phases apatite and perhaps tantalite-columbite. The removal of these phases from the melt is noted in many instances by the inverse kinks of Nd and Dy in later-stage minerals.

To test whether the trace-element data are consistent with (Rayleigh) fractional crystallization, the behavior of Rb and Sr through the sequential crystallization of the wall zone and first intermediate zone followed by simultaneous crystallization of the remaining zones is examined in Figure 16. The composition of the estimated initial parent melt (Table 6) is used as the starting composition. The trend is similar for equilibrium crystallization, although the rate of enrichment of Rb and depletion of Sr along the crystallization path is less.

The trace-element data are inconsistent with the crystallization model, although the composition of the melt does show progressive enrichment of Rb and depletion of Sr. The major discrepancy with the model is that parts of the third intermediate zone and core apparently crystallized from a more Rb-depleted melt than did the first and second intermediate zones. The extremely high concentrations of Rb within the first and second intermediate zones, and the crystallization of pollucite near the end of second-intermediate-zone crystallization, may indicate that Rb and Cs were transported upward within an exsolved aqueous-fluid phase, mimicking the vertical zonation of

K and Na. A similar enrichment process was suggested to explain Rb enrichments in the pegmatitic granites examined by Goad and Černý (1981). The large discrepancies between the calculated melt compositions and the model are probably the result of the qualitative nature of the distribution coefficients.

Origin of zoning

Zonations within the pegmatite were probably not a result of interactions of the melt and fluid of the pegmatite with the country rocks. The worldwide similarity of zoned pegmatites intruding a variety of rock types argues against such interaction being a dominant process.

Two possible closed-system mechanisms for producing zonations consistent with the crystallization sequence determined are (1) the minimum melt composition of the system was abruptly altered, leaving the composition of the melt offset from the minimum composition of the system, or (2) a minimum melt composition was retained throughout crystallization of each zone but was chemically buffered by the crystallization of corresponding phases in other zones, facilitated by the rapid mass transport capabilities of a coexisting fluid phase.

The abrupt addition of halogens to a melt, or removal of halogens from melt into an exsolving aqueous- or carbonate-rich-fluid phase, may change the minimum melt composition of the system (Kovalenko, 1978; Manning, 1981), requiring that the melt evolve toward its new minimum melt composition. For example, the sudden removal of F or Cl from a granite melt may change the minimum melt composition of the system to a more quartz- and orthoclase-rich composition (Manning, 1981). An albite-rich assemblage would then crystallize as the melt composition evolved to its new minimum melt composition. The alteration of the minimum melt composition may result in the crystallization of some assemblages observed in zoned pegmatites. Although vertical stratification resulting from compositional gradients of halogens within the melt-fluid system probably could only be maintained for a small proportion of the crystallization of a pegmatite, it is possible that the redistribution of F or Cl within a pegmatite may start other compositional gradients that could continue throughout the crystallization sequence.

Internal buffering of the melt near the minimum composition via a fluid phase may explain the vertical zonation. The movement of elements within a fluid and crystallization of material from a fluid are likely to be extremely rapid relative to diffusion within the melt, exchange with crystals, or crystallization from the melt. As discussed by Jahns and Burnham (1969), an exsolved fluid likely rises quickly within a granitic melt and possibly pools in the upper regions of the crystallizing body because of the extreme density contrast between the melt and fluid. Burnham (1967) calculated that aqueous bubbles might rise through a granitic melt as rapidly as 125 cm/yr, which is much more rapid than diffusion within a melt (for example 1.94 cm/yr for potassium at 700°C; Jambon, 1982).

Table 6. Calculated trace alkali and alkaline-earth concentrations in three parent melts for whole-rock samples of wall zone

Sample #*	9-2	10-3	43-1
Calculated parent melt (ppm)			
Rb	3630	2230	6990
Cs	684	1660	3010
Li	5900	4000	10000
Sr	18	40	23
Ba	41	84	59

* see Table 2 for compositional data.

Thus, the rising fluid might stratify the melt with respect to elements with melt/fluid partition coefficients of less than one. Sakugama and Kushiro (1979) experimentally demonstrated that an aqueous-fluid phase exsolved from an andesitic melt can stratify a melt with respect to Na and K by transporting the elements upward as the fluid rises.

It has also been proposed by Jahns and Burnham (1969) and Jahns (1982) that fluids might coat the surfaces of minerals forming on the inner crystallization surfaces of a pegmatite. If the surficial coatings form an interconnected network in the body, the fluid will provide a mechanism for movement of material throughout the crystallizing body.

In early studies, Norton et al. (1962) and Jahns and Tuttle (1963) speculated that the vertical zonation observed in pegmatites is the result of the upward transport of K relative to Na by exsolving fluids. The exsolution of K-rich fluids, however, was found to be inconsistent with both the experimentally determined partition coefficients of alkalis between a granitic melt and aqueous fluids, and the alkali contents of fluid inclusions. The results of Orville (1963), Hemley (1967), and Holland (1972) and a fluid-inclusion study by Horn and Wickman (1973) have shown that fluid/mineral and fluid/melt partition coefficients are larger for Na than K.

Although one-way preferential movement of K relative to Na is unlikely, several properties of aqueous fluids suggest that fluids might serve as very efficient two-way pathways to move and redistribute material within a crystallizing granitic system. The fluid/melt distribution coefficients of K and Na determined by Holland (1972) indicate that significant concentrations of alkalis can partition into an aqueous fluid if the fluid has relatively high chlorinities. K has a fluid/melt partition coefficient greater than 1.0 for fluids with greater than 3.0 molal Cl, while Na fluid/melt partition coefficients are greater than 1.0 for fluids with molalities of only 2.2 and greater. Cl molalities of 1-4 are likely within a highly differentiated magmatic system because Cl partitions almost exclusively into aqueous fluid relative to a silicate melt (Burnham, 1967, 1979). Luth and Tuttle (1969) suggested that significant concentrations of SiO₂ might also be incorporated into an aqueous fluid. Thus, an exsolving aqueous fluid can re-

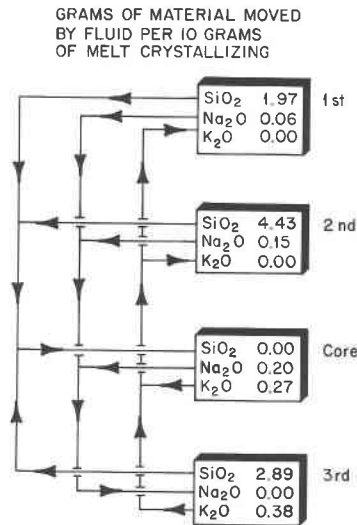


Fig. 17. Schematic diagram showing the amounts of three main oxides that would have to be transferred from one part of the pegmatite to another in order to retain a single minimum melt composition of SiO₂ = 76.22 wt%, Al₂O₃ = 15.56 wt%, Na₂O = 3.62 wt%, K₂O = 4.18 wt% throughout the pegmatite. Material transfer occurs via an interconnected fluid phase (see text for discussion).

move Si, Na, and K from a coexisting silicate melt and transport the material to another part of the pegmatite, requiring crystallization of a nonminimum composition assemblage. These elements might constitute greater than 5–10 wt% of the total fluid.

Similar models of fluid transport have been considered by Jahns (1956) and others to explain the occurrence of quartz cores in pegmatites. For a fluid to have redistributed material within a pegmatite and produced the compositional variations noted in the Tin Mountain pegmatite, the fluid would have had to transfer Si and Na from the crystallization fronts of the first two intermediate zones to the core and third intermediate zones, respectively, where these constituents would have been incorporated into crystallizing phases. Similarly, the fluid would have had to transfer Si to the core and K to the first and second intermediate zones from the crystallizing front of the third intermediate zone. The mechanism driving the vertical transport may have been the rapid growth of K-feldspar in the upper part of the pegmatite relative to the rate of growth of albite in the lower part of the pegmatite, resulting in chemical potential gradients in the fluid. Other possible mechanisms include temperature (as was discussed by Orville, 1963), pressure, gravity, and halogen gradients within the body.

If the minimum melt composition of the total pegmatite system remained constant throughout crystallization, the amount of material required to be transported by fluids can be estimated. The amount of each element entering the fluid phase during crystallization is determined by subtracting the maximum amount of each element that

Table 7. Mass (in grams) of four oxides that can be incorporated into the lithology of each zone and the mass of excess material that must be removed by a fluid phase to retain the minimum melt composition, for each 10 g of melt crystallizing

Oxide (g)	SiO ₂	Al ₂ O ₃	Na ₂ O	K ₂ O	H ₂ O
ZONE					
1ST Int					
Rock	4.87	0.95	0.21	0.44	0.00
Excess	1.97	0.45	0.06	0.00	1.00
2ND Int					
Rock	2.34	0.64	0.10	0.39	0.00
Excess	4.43	0.79	0.15	0.00	1.00
3RD Int					
Rock	4.18	0.90	0.27	0.01	0.00
Excess	2.66	0.50	0.00	0.42	1.00
Core					
Rock	6.80	1.06	0.07	0.12	0.00
Excess	0.00	0.37	0.20	0.27	1.00

can be removed from the melt by crystallization from the composition of the minimum melt. Mass-balance calculations for each zone were done using a minimum melt composition of 76.22 wt% SiO₂, 15.56 wt% Al₂O₃, 3.62 wt% Na₂O, and 4.18 wt% K₂O, which is the estimated composition of the melt after crystallization of the wall zone. The model assumes crystallization of rock with the modal mineralogy of each of the four inner zones (Table 1) and 10 wt% saturation of the melt with water (Table 7). The calculated masses of transported elements are the maximum because some amount of each element may have been transported from the other crystallization fronts of the other zones and because the percentage of fluid relative to melt will increase as crystallization proceeds. Figure 17 illustrates the requisite paths for mass transfer and the grams of each element that had to be removed from each of the four crystallization fronts and transferred elsewhere by fluid for each 10 g of melt crystallizing.

The results suggest that most material removed from the crystallizing melt went into the production of minerals, but also that a significant amount of silicate material would have had to enter the fluid at one crystallizing front and move through the fluid to another location where it was deposited. The connecting aqueous fluid had to remain undersaturated with respect to silicates along the crystallization fronts. Because of the rapid transfer capabilities of a fluid relative to a crystallizing melt, large volumes of fluid were not necessary, provided excess silicate material was deposited in other zones.

As noted, the second intermediate zone probably crystallized simultaneously with the spodumene-bearing third intermediate zone and core, so that the melt from which it crystallized would have been saturated with spodumene. The absence of spodumene in the second intermediate zone suggests that Li was removed from the crystallization front of that zone and was transferred downward. However, the data for evaluating the behavior of Li in a fluid are not available.

SUMMARY

(1) The lithologic zones of the Tin Mountain pegmatite resulted from crystal-melt and crystal-aqueous-fluid frac-

tionation and fluid-assisted compositional stratification. (2) The wall zone crystallized first. This is indicated by its geothermometry and low concentrations of Rb, Cs, and Li, high concentrations of Sr and Ba, and REE patterns indicating crystal accumulation. (3) The K-rich first intermediate zone crystallized following the wall zone in the crystallization sequence. High concentrations of Sr and positive Eu anomalies in feldspars argue for early crystallization relative to the three remaining inner zones. (4) Either the structure of the melt changed or the melt-fluid system became highly oxidizing after the crystallization of the first intermediate zone, resulting in the formation of predominately Eu^{3+} , as indicated by the absence of positive Eu anomalies in the feldspars of the remaining zones. (5) Geothermometry and Sr data combined with REE data suggest that the core and the second and third intermediate zones crystallized simultaneously toward the central parts of the pegmatite. (6) The melt-fluid system that crystallized to form the inner zones may have become vertically segregated with respect to Rb, Cs, and Li because of fluid transport. Fluid transport also continually supplied the crystallization fronts of the first and second intermediate zones with K (and continually removed Na and Li), and conversely, the core and third intermediate zone were supplied with Na, Li, and Si. The mechanism driving the material transport remains elusive, but chemical potential gradients in major elements or halogens, gravitational gradient, pressure gradient, or temperature gradient within the body could potentially have driven the movement.

ACKNOWLEDGMENTS

Petr Černý and two anonymous reviewers are thanked for substantially improving this manuscript. Earlier drafts of this manuscript benefitted from the reviews of P. I. Nabelek, J. A. Redden, and J. J. Norton. Eugene Foord is thanked for analyzing apatites for F, Cl, and OH. Lois Koh is acknowledged for drafting many of the figures. Funding was provided by DOE contracts DE-AC02-79ER-10412 and DE-AC01-82ER-12040 and DOE grant DE-FG01-84ER-13259. Additional funding was provided by a fellowship from the Northwest College and University Association for Science. These sources of funding are gratefully acknowledged.

REFERENCES

- Albee, A.L., and Ray, L. (1970) Correction factors for electron probe micro-analysis of silicates, oxides, carbonates, phosphates and sulfates. *Analytical Chemistry*, 42, 1408–1414.
- Arth, J.G. (1976) Behavior of trace elements during magmatic processes—A summary of the theoretical models and their applications. *U.S. Geological Survey Journal of Research*, 4, 41–47.
- Bence, A.E., Albee, A.L. (1968) Empirical correction factors for electron microanalysis of silicates and oxides. *Journal of Geology*, 76, 382–403.
- Bottinga, Y., and Javoy, M. (1975) Oxygen isotope partitioning among the minerals in igneous and metamorphic rocks. *Reviews of Geophysics and Space Physics*, 13, 401–418.
- Brookins, D.G., Fairbairn, H.W., Hurley, P.M., and Pinson, W.H. (1969) A Rb-Sr geochronologic study of the pegmatites of the Middletown area, Connecticut. *Contributions to Mineralogy and Petrology*, 22, 157–168.
- Brown, W.L., and Parsons, Ian. (1981) Towards a more practical two-feldspar geothermometer. *Contributions to Mineralogy and Petrology*, 76, 369–377.
- Burnham, C.W. (1963) Viscosity of a water-rich pegmatite melt at high pressures. *Geological Society of America Special Paper* 76, 26.
- (1967) Hydrothermal fluids at the magmatic stage. In H. L. Barnes, Ed., *Geochemistry of hydrothermal ore deposits*, 34–76. Holt, Reinhart and Winston, New York.
- (1979) Magmas and hydrothermal fluids. In H. L. Barnes, Ed., *Geochemistry of hydrothermal ore deposits*, 2nd edition, 71–136. Wiley, New York.
- Burnham, C.W., and Jahns, R.H. (1962) A method for determining the solubility of water in silicate melts. *American Journal of Science*, 260, 721–745.
- Cameron, E.N., Jahns, R.H., McNair, A.H., and Page, L.R. (1949) Internal structure of granitic pegmatites. *Economic Geology Monograph* 2.
- Carron, J.-P., and Lagache, Martine. (1980) Etude expérimentale du fractionnement des éléments Rb, Cs, Sr, et Ba entre feldspaths alcalins, solutions hydrothermales et liquides silicatés dans le système $\text{Q.Ab.Or.H}_2\text{O}$ à 2 Kbar entre 700 et 800°C. *Bulletin de Minéralogie*, 103, 571–578.
- Černá, I., Černý, Petr, and Ferguson, R.B. (1972) The Tanco pegmatite at Bernic Lake, Manitoba. III. Amblygonite-montebrazite. *Canadian Mineralogist*, 11, 643–659.
- Černý, Petr, Smith, J.V., Mason, R.A. and Delaney J.S. (1984) Geochemistry and petrology of feldspar crystallization in the Vezna pegmatite, Czechoslovakia. *Canadian Mineralogist*, 22, 631–651.
- Chatterjee, A.K., and Strong, D.F. (1984) Rare earth and other element variations in greisens and granites associated with east Kemptville tin deposit, Nova Scotia, Canada. *Institute of Mining and Metallurgy Transactions, Section B*, 93, 59–70.
- Coats, R.R. (1956) Uranium and certain other trace elements in feldic volcanic rocks of Cenozoic age in Western United States. *U.S. Geological Survey Professional Paper* 300.
- DeVoto, R.H. (1978) Uranium geology and exploration—Lecture notes and references. *Colorado School of Mines, Golden, Colorado*.
- Drake, M.J., and Weill, D.F. (1975) Partition of Sr, Ba, Ca, Y, Eu^{2+} , Eu^{3+} , and other REE between plagioclase feldspar and magmatic liquid: An experimental study. *Geochimica et Cosmochimica Acta*, 39, 689–712.
- Glyuk, D.S., and Trufanova, L.G. (1978) Melting at 1000 Kg/cm^2 in a granite- H_2O system with the addition of HF, HCl, and Li, Na, and K fluorides, chlorides, and hydroxides. *Geochemistry International*, 14, 28–36.
- Goad, B.E., and Černý, Petr. (1981) Peraluminous pegmatitic granites and their pegmatite aureoles in the Winnipeg River district, southeastern Manitoba. *Canadian Mineralogist*, 19, 177–194.
- Gromet, L.P., and Silver, L.T. (1983) Rare earth element distributions among minerals in a granodiorite and their petrogenetic implications. *Geochimica et Cosmochimica Acta*, 47, 925–939.
- Hanson, G.N. (1980) Rare earth elements in petrogenetic studies of igneous systems. *Annual Reviews of the Earth and Planetary Sciences*, 8, 371–406.
- Harris, N.B.W., and Marriner, G.F. (1980) Geochemistry and petrogenesis of a peralkaline granite complex from the Midian Mountains, Saudi Arabia. *Lithos*, 13, 325–337.
- Hemley, J.J. (1967) Aqueous Na/K ratios in the system $\text{K}_2\text{O-Na}_2\text{O-Al}_2\text{O}_3\text{-SiO}_2\text{-H}_2\text{O}$. *Geological Society of America Abstracts with Programs*, 94–95.
- Hildreth, E.W. (1977) The magma chamber of the Bishop Tuff: Gradients in temperature, pressure and composition. Ph.D. thesis, University of California, Berkeley.
- Holland, H.D. (1972) Granites, solutions and base metal deposits. *Economic Geology*, 67, 281–301.
- Horn, R.A., and Wickman, F.E. (1973) The Na/K ratio of fluid

- inclusions in pegmatitic quartz and its genetic implications. A study by neutron activation analysis. *Lithos*, 6, 373-387.
- Hudson, Travis, and Arth, J.G. (1983) Tin granites of the Seward Peninsula, Alaska. *Geological Society of America Bulletin* 94, 768-790.
- Jahns, R.H. (1956) Resurgent boiling and the formation of magmatic pegmatites. *Geological Society of America Bulletin* 67, 1772.
- (1982) Internal evolution of pegmatite bodies. In P. Černý, Ed. *Granitic pegmatites in science and industry*, 293-327. Mineralogical Association of Canada Short Course Handbook 8.
- Jahns, R.H., and Burnham, C.W. (1957) Preliminary results from experimental melting and crystallization of Harding, New Mexico, pegmatite. *Geological Society of America Bulletin* 68, 1751-1752.
- (1969) Experimental studies of pegmatite genesis: 1. A model for the derivation and crystallization of granite pegmatites. *Economic Geology*, 64, 843-864.
- Jahns, R.H., and Tuttle, O.F. (1963) Layered pegmatite aplite intrusives. *Mineralogical Society of America Special Paper* 1, 78-92.
- Jambon, A. (1982) Tracer diffusion in granitic melts: Experimental results for Na, K, Rb, Cs, Ca, Sr, Ba, Ce, Eu to 1300°C and a model of calculation. *Journal of Geophysical Research*, 87, 10 797-10 810.
- Kovalenko, N.I. (1978) The reactions between granite and aqueous hydrofluoric acid in relation to the origin of fluorine-bearing granites. *Geochemistry International*, 14, 108-118.
- Laul, J.C. (1979) Neutron activation analysis of geological materials. *Atomic Energy Review*, 17, 603-695.
- London, David, and Burt, D.M. (1982) Chemical models for lithium aluminosilicate stabilities in pegmatites and granites. *American Mineralogist*, 67, 494-509.
- Longstaffe, F.J., Černý, P., and Muehlenbachs, K. (1981) Oxygen-isotope geochemistry of the granitoid rocks in the Winnipeg River Pegmatite District, southeastern Manitoba. *Canadian Mineralogist*, 19, 195-204.
- Luth, W.C., and Tuttle, O.F. (1969) The hydrous vapor phase in equilibrium with granite and granite magmas. *Geological Society of America Memoir* 115, 513-548.
- Manning, D.A.C. (1981) The effect of fluorine on liquidus phase relationships in the system Qz-Ab-Or with excess water at 1 Kb. *Contributions to Mineralogy and Petrology*, 76, 206-215.
- Miller, C.F., and Mittlefehldt, D.W. (1982) Depletion of light rare-earth elements in felsic magmas. *Geology*, 10, 129-133.
- Minyev, D.A. (1963) Geochemical differentiation of rare earths. *Geochemistry*, 1129-1149.
- Möller, P., and Muecke, G.K. (1984) Significance of europium anomalies in silicate melts and crystal-melt equilibria: A re-evaluation. *Contributions to Mineralogy and Petrology*, 87, 242-250.
- Norton, J.J. (1983) Sequence of mineral assemblages in differentiated granitic pegmatites. *Economic Geology*, 78, 854-874.
- Norton, J.J., Page, L.R., and Brobst, D.A. (1962) Geology of the Hugo pegmatite, Keystone, South Dakota. U.S. Geological Survey Professional Paper 297-B, 49-126.
- Orville, P.M. (1960) Petrology of several pegmatites in the Keystone District, Black Hills, S.D. *Geological Society of America Bulletin*, 71, 1467-1490.
- (1963) Alkali ion exchange between vapor and feldspar phases. *American Journal of Science* 261, 201-237.
- Papike, J.J., Shearer, C.K., Simon, S.B., and Laul, J.C. (1983) Fluid flow through crystalline rocks: Sheet silicates as trace element traps. *Geological Society of America Abstracts with Programs*, 15, 658.
- Pichavant, Michel. (1981) An experimental study of the effect of boron on a water-saturated haplogranite at 1 kbar vapour pressure. *Contributions to Mineralogy and Petrology* 76, 430-439.
- Redden, J.A. (1963) Geology and pegmatites of the Fourmile quadrangle, Black Hills, South Dakota. U.S. Geological Survey Professional Paper 297-D.
- Redden, J.A., Norton, J.J., and McLaughlin, R.J. (1982) Geology of the Harney Peak Granite, Black Hills, South Dakota. U.S. Geological Survey Open-File Report 82-481.
- Register, M.E. (1979) Geochemistry and geochronology of the Harding pegmatite, Taos County, New Mexico. M.S. thesis, University of New Mexico, Albuquerque.
- Riley, G.H. (1970) Isotopic discrepancies in zoned pegmatites, Black Hills, South Dakota. *Geochemica et Cosmochimica Acta*, 34, 713-725.
- Rogers, J.W. (1964) Statistical tests of the homogeneity of the radioactive components of granitic rocks. In J.A.S. Adams and W.M. Lowder, Eds. *The natural radiation environment*, 51, Chicago University Press, Chicago.
- Rogers, J.J.W., and Adams, J.A.S. (1969) Uranium. In K.H. Wedepohl, Ed. *Handbook of geochemistry*, volume 2, number 1, Springer-Verlag, New York.
- Sakuyama, M., and Kushihiro, I. (1979) Vesiculation of hydrous andesitic melt and transport of alkalis by separated vapor phase. *Contributions to Mineralogy and Petrology*, 71, 61-66.
- Shearer, C.K., Papike, J.J., Redden, J.A., and Walker, R.J. (1984) Mineralogy and REE geochemistry of an S-type granite: The Harney Peak Granite. *Geological Society of America Abstracts with Programs*, 16, 652.
- Shirey, S.B. (1984) The origin of Archean crust in the Rainy Lake area, Ontario. Ph.D. dissertation, State University of New York at Stony Brook.
- Shmakin, B.M. (1979) Composition and structural state of K-feldspars from some U.S. pegmatites. *American Mineralogist*, 64, 49-56.
- Staatz, M.H., Murata, K.J., and Glass, J.S. (1955) Variation of composition and physical properties of tourmaline with its position in the pegmatite. *American Mineralogist*, 40, 789-804.
- Staatz, M.H., Page, L.R., Norton, J.J., and Wilmarth, V.R. (1963) Exploration for beryllium at the Helen Beryl, Elkhorn, and Tin Mountain pegmatites, Custer County, South Dakota. U.S. Geological Survey Professional Paper 297-C.
- Stewart, D.B. (1960) The system $\text{LiAlSi}_4\text{O}_8\text{-NaAlSi}_3\text{O}_8\text{-H}_2\text{O}$ at 2000 bars. In *Minerals and genesis of pegmatites*. 21st International Geological Congress, Copenhagen, 1960, 15-30.
- (1978) Petrogenesis of lithium-rich pegmatites. *American Mineralogist*, 63, 970-980.
- Strong, D.F., Fryer, B.J., and Kerrich, R. (1984) Genesis of the St. Lawrence fluor spar deposits as indicated by fluid inclusion, rare earth element, and isotopic data. *Economic Geology*, 79, 1142-1158.
- Taylor, B.E., and Friedrichsen, Hans. (1983a) Light stable isotope systematics of granitic pegmatites from North America and Norway. *Isotope Geoscience*, 1, 127-167.
- (1983b) Oxygen and hydrogen isotope disequilibria in the Landsverk I pegmatite, Evje, southern Norway: Evidence for anomalous hydrothermal fluids. *Norsk Geologisk Tidsskrift*, 6, 199-209.
- Taylor, B.E., Foord, E.E., and Friedrichsen, Hans. (1979) Stable isotopes and fluid-inclusion studies of gem-bearing granitic pegmatite-aplite dikes, San Diego Co., California. *Contributions to Mineralogy and Petrology*, 68, 187-205.
- Taylor, H.P. (1968) The oxygen isotope geochemistry of igneous rocks. *Contributions to Mineralogy and Petrology*, 19, 1-71.
- Turekian, K.K., and Wedepohl, K.H. (1961) Distribution of the elements in some major units of the Earth's crust. *Geological Society of America Bulletin*, 72, 1723-1728.
- Uebel, P.-J. (1977) Internal structure of pegmatites, its origin and nomenclature. *Neues Jahrbuch für Mineralogie Abhandlungen*, 131, 83-113.
- Volfinger, Marcel, and Robert, J.-L. (1980) Structural control of the distribution of trace elements between silicates and hydrothermal solutions. *Geochimica et Cosmochimica Acta*, 44, 1455-1461.
- Walker, R.J. (1984) Origin of the Tin Mountain Pegmatite, Black

- Hills, South Dakota. Ph.D. dissertation, State University of New York at Stony Brook.
- Walker, R.J., Papike, J.J., and Hanson, G.N. (1985) Fractionation within a granitic system: The Harney Peak Granite, Black Hills, South Dakota. EOS (American Geophysical Union Transactions), 66, 415.
- Weis, P.L. (1953) Fluid inclusions in minerals from zoned pegmatites of the Black Hills, South Dakota. American Mineralogist, 38, 671-697.
- Whitney, J.A., and Stormer, J.C. (1977) The distribution of $\text{NaAlSi}_3\text{O}_8$ between coexisting microcline and plagioclase and its effect on geothermometric calculations. American Mineralogist, 62, 687-691.
- Windrim, D.P., McCulloch, M.T., Chappell, B.W., and Cameron, W.E. (1984) Nd isotopic systematics and chemistry of Central Australian sapphirine granulites: An example of rare earth mobility. Earth and Planetary Science Letters, 70, 27-39.

MANUSCRIPT RECEIVED FEBRUARY 28, 1985

MANUSCRIPT ACCEPTED NOVEMBER 15, 1985